CHALMERS
UNIVERSITY OF TECHNOLOGY

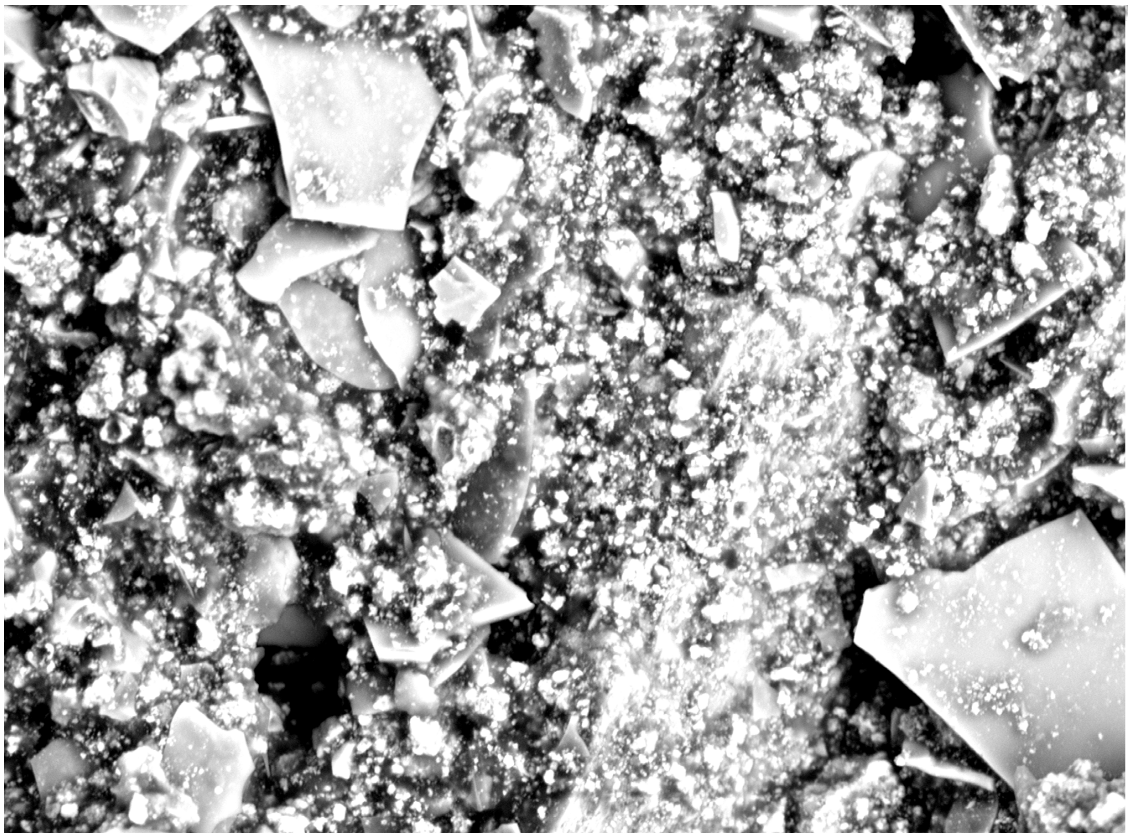

Investigation of sodium trapped by the filter cake during separation of iron from sewage sludge ash

Cause of the losses and influence of extensive washing

Master's thesis in Innovative and Sustainable Chemical Engineering

My Dahlbom Järvinen and Emmy Mäkitalo

DEPARTMENT OF CHEMISTRY AND CHEMICAL ENGINEERING
CHALMERS UNIVERSITY OF TECHNOLOGY
Gothenburg, Sweden 2021
www.chalmers.se

Master's thesis 2021

Investigation of sodium trapped by the filter cake during separation of iron from sewage sludge ash

Cause of the losses and influence of extensive washing

My Dahlbom Järvinen and Emmy Mäkitalo

CHALMERS
UNIVERSITY OF TECHNOLOGY

Department of Chemistry and Chemical Engineering
Division of Energy and Materials
Chalmers University of Technology
Gothenburg, Sweden 2021

Investigation of sodium trapped by the filter cake during separation of iron from sewage sludge ash
- Cause of the losses and influence of extensive washing
My Dahlbom Järvinen and Emmy Mäkitalo

Supervisors:
Liubov Vasenko, Process Engineer, EasyMining Sweden AB
Harshad Pathak, Chemical Process Development Engineer, EasyMining Sweden AB
Pavleta Knutsson, Associate Professor, Department of Chemistry and Chemical Engineering, Chalmers University of Technology

Examiner:
Britt-Marie Steenari, Professor, Department of Chemistry and Chemical Engineering, Chalmers University of Technology

Master's Thesis 2021
Department of Chemistry and Chemical Engineering
Division of Energy and Materials
Chalmers University of Technology
SE-412 96 Gothenburg
Telephone +46 31 772 1000

Cover: SEM-micrograph of filter cake particles obtained from the iron separation.

Typeset in LaTeX, template by Magnus Gustaver

Investigation of sodium trapped by the filter cake during separation of iron from sewage sludge ash
- Cause of the losses and influence of extensive washing
My Dahlbom Järvinen and Emmy Mäkitalo
Department of Chemistry and Chemical Engineering
Chalmers University of Technology

Abstract

The company EasyMining has developed a process, Ash2Phos, to recover P from incinerated sewage sludge ash. The purpose of this report was to investigate the cause of Na losses to the filter cake during separation of Fe in one of the process steps. The project also aimed at exploring the influence of washing on the Na losses. The investigation was done by conducting a process reproduction experiment on a semi-pilot scale, including cycles with different washing conditions. Since the focus of the project was the Fe separation step, the experimental setup was simplified compared to the large scale process and did only include upstream process steps. The evaluation of Na losses to the filter cake and the influence of washing were done by constructing a mass balance, based on analyses with ICP-AES and ICP-MS, over the process step for the cycles with different washing conditions. The evaluation of the filter cake composition and elemental distribution was conducted by SEM-EDS analysis on filter cakes with different washing conditions. Analysis with XRD was also performed to investigate possible crystalline structures containing Na. Additional experiments on lab scale were performed on one of the known filter cake components, Al-silicates, to study its adsorption potential, washing behaviour and influence on the Na losses. The studies identified three main Na containing particles in the filter cake: Fe-precipitates, Al-silicates and Ca-precipitates. Extensive washing was found to be efficient for Na removal from the filter cake, however, only to a limited extent. Further, it was not possible to identify any crystalline structures containing Na. Based on the lab scale experiment, the losses of Na to the Al-silicates were not due to adsorption, instead it was related to trapped liquid in the cake. Finally, Fe-precipitates were identified as the main contributors to the Na losses but further studies are required to identify the mechanism and reduce the losses. It would also be of great interest to optimise the washing by including a cost perspective and large scale process conditions.

Keywords: sodium losses, filter cake washing, adsorption of sodium, phosphorus recovery, sewage sludge ash.

Acknowledgements

We are grateful for everyone that has been involved in this thesis project. It would not have been possible without your practical help and deep knowledge. First of all, we want to thank EasyMining for giving us the opportunity and trust of performing this task. To Ida Blomgren and Liubov Vasenko from EasyMining, thank you for introducing us to the subject and believing in our abilities from the start. We also want to give an extra thank you to our supervisor from EasyMining, Liubov Vasenko, for introducing us to the process, for your help with planning and conducting the experiments, for your dedication to the project and for your support and constant feedback throughout the entire process. Thank you also to our supervisor from EasyMining, Harshad Pathak, for your guidance during the planning, preparation and performance of the experiments and for your support during our stay in Uppsala. To Yariv Cohen, thank you for your input and help to re-plan the experiments in such short notice. Thank you to both EasyMining teams in Gothenburg and Uppsala for your warm welcome. For the team in Uppsala, we are also grateful for getting access to your lab and for your kind help whenever it was needed. We also want to thank our examiner Professor Britt-Marie Steenari and our supervisor Associate Professor Pavleta Knutsson from Chalmers University of Technology for your commitment, academic expertise and insightful input which improved the investigation significantly. Finally, thank you to Liubov Vasenko, Pavleta Knutsson and Ida Blomgren for you rewarding feedback on the content of the report.

My Dahlbom Järvinen and Emmy Mäkitalo, Gothenburg, June 2021

Contents

List of Figures

List of Tables

1
Introduction

1.1 Background

P is an essential chemical element for all living cells and the P supply to agriculture is essential for global food production [1]. Due to a rising population and a globally changing diet with an increasing meat consumption, the demand of P in agriculture is continuously growing [2]. Today, P is mainly mined from phosphate rocks and according to the International Fertiliser Association (IFA) [3], at least 80% of the global output of mined phosphate rock is used for production of P-fertilisers. Besides the use of P in the fertiliser industry, it is also used in several applications in chemical and food industry [4]. However, since mined P is a limited, nonrenewable resource that is only available in a number of countries, there is a global interest to both find more sustainable produced P and to secure access for countries that lack phosphate deposits [2]. One solution to secure access to more sustainable generated P, is to increase the recovery and recycling from organic waste flows generated by human activities. In that way, the demand and dependency of mining from phosphate rocks will be reduced [5]. Examples of suitable waste flows in society are wastewater, livestock manure, food waste and food processing residues that possibly could be used as sources of P in the near future [1].

A possible method to recover P is to recirculate it from sewage sludge from the wastewater treatment system [2]. The sewage sludge can directly be spread on agricultural land, but it is common to incinerate the sludge in order to reduce the volume, and by that the cost for transportation [6]. Incineration can also be motivated by legislation that prohibits landfilling in some countries [7]. By incinerating the sewage sludge, the nutrient concentration is increased and the risk for contamination of the soil from pathogens in the sludge is reduced. It is also possible to reduce the amounts of heavy metals by extracting P in concentrated form from the sewage sludge ash [6]. By further removing Al and Fe, a high quality of the P enriched product can be obtained [8].

EasyMining has developed a technology, called Ash2Phos, where P is recovered from incinerated sewage sludge ash in several steps [9]. The ash is firstly treated in acid to dissolve major constituents. Recoverable elements are thereafter separated from the dissolved sewage sludge ash and are finally being converted into valuable P, Fe and Al products in several steps. In the separation of Fe, a reactor is filled with an acidic stream containing mostly Fe, P and Al as well as some minor elements from

the ash. NaOH is also added to trigger Fe precipitation. The slurry is thereafter filtered into a solid filter cake containing Fe and a liquid phase containing P, Al and Na. The liquid phase is further treated to recover P and Al as separate product streams, while the intention is to recover Na from downstream process steps and recirculate it back to the reactor.

During the filtration Na is, however, partly trapped in the filter cake together with the Fe, resulting in an increased requirement for expensive NaOH make-up. This results in an increased operational cost and a decrease in resource efficiency. Since both a reaction stage and a filtration stage is part of the separation of Fe, several causes of the losses are possible. The reaction conditions, which aims at the dissolution of P and precipitation of Fe at high pH, can possibly lead to the formation of other undesired Na containing solid compounds which are problematic to remove. The following filtration stage, which involves vacuum filtration followed by washing of the filter cake, can be hindered by several factors such as undesired Na adsorption on filter cake components or a tortuous pore system [10]. These potential causes need to be investigated in order to estimate the extent of the problematic losses and evaluate possibilities of minimising them in a feasible way.

1.2 Aim

The aim of the thesis is to study possible causes of undesired Na losses during separation of Fe. The investigations is mainly based on reproducing a part of the process on a semi-pilot scale and produce filter cakes representative to the large scale process. The composition of the filter cake as well as the filter cake components will be explored and the presence of solid compounds that directly or indirectly can affect the Na losses will be investigated. Finally, the effect of varying washing conditions on the filter cake composition, with a special focus on the Na content, will be evaluated in order to draw conclusions regarding future optimisation strategies.

1.3 Limitations

The investigation was mainly limited by the possibility of reproducing the large scale process step on a semi-pilot scale as representative as possible with respect to Na losses within the limited scope of the project. The restriction introduced were those on elements distribution and process steps, stated below.

1.3.1 Restrictions on elements

The main objective of the investigation was to evaluate possible mechanism responsible for the Na losses in the separation of Fe step. Therefore, the focus of the experiments were to evaluate the reaction and filtration efficiency with respect to Na content in the filter cake. The behaviour of other elements and the effect of washing on them and are not investigated.

1.3.2 Restrictions on process steps

The prior process steps to the Fe separation step were included in the experimental part in a modified form but these are not a central part of the discussion. Downstream steps were not conducted and recirculating streams from these were instead mimicked by addition of an artificial solution. Due to some of the deviations from the large scale process, only the mechanisms and the trends of the Na losses can be determined.

2
Theory

This chapter starts with a more detailed input regarding the importance of a circular P system which serves as background to the need of the Ash2Phos process. An overview of the process is thereafter presented followed by a more detailed description of the separation of Fe and the theory behind the operations involved. Finally, possible mechanisms responsible for losses during filtration and washing are provided as well.

2.1 Phosphorus theory

P is a finite resource that is essential for global food production and the interest is growing of finding more sustainable and efficient sources of P than virgin extraction. A potential source of P is to use organic waste flows generated by human activities, where especially sewage sludge from wastewater is of high interest. In this section, an overview of virgin extraction of P and examples of common production routes for different P products are presented. This section also provides an introduction to sewage sludge treatment and examples of possible strategies for recovery of nutrients from sewage sludge.

2.1.1 Virgin extraction of phosphorus

Today, P is mainly produced by mining of phosphate rocks, and the main suppliers are China, Morocco, United States, and Russia. The largest known reserves are located in Morocco and Western Sahara and they account for 70-75 % of the global available reserves [4],[11]. As with all mining activities of limited resources, the extraction and processing of phosphate rock, is linked to several environmental impacts. Locally, the mining can cause water contamination due to release of process water or leaching of process waste. It can also be linked to an excessive water consumption and disturbances to the local landscape [12]. Further, mining is related to generation of emissions such as dust and greenhouse gases, where the latter may contribute to global warming [12],[13]. The mining does also result in generation of large hidden waste flows.

The uneven distribution of P resources in the world results in a large dependency of import for many countries. In Europe, only a small share of the P demand is covered by local manufacturing, meanwhile the majority is dependent on import. According to the European Commission, the import reliance of phosphate rock for

the European Union was 84 % in 2020 [14]. Due to the lack of efficient P sources in Europe, the European Commission decided to add phosphate rock to their list of critical raw materials [4]. Thus, phosphate rock is included in the action plan for critical raw materials, where the focus is put on diversifying the supply, improving resource efficiency as well as increased recycling [14].

2.1.2 Intermediary products of phosphorus

Extracted phosphate rock is typically processed into two main intermediary products, H_3PO_4 and P_4 [15]. Together, these compounds form the basis of the P chemistry. H_3PO_4 is closely related to the production of fertilisers and P_4 is the starting material for several high-grade P products, with both industrial and food applications [4]. H_3PO_4 is typically produced through the wet process, which is the most common treatment method applied today. The process consists of digestion of phosphate rock by addition of concentrated H_2SO_4, followed by removal of $CaSO_4$ by filtration. In order to be able to further process it into fertiliser products, it is commonly required to reduce the liquid content of the product and purify them from other inorganic compounds [16]. P_4 is generated through reduction of phosphates at elevated temperatures and it is primarily done by the Wöhler process [4].

2.1.3 Phosphorus recovery from sewage sludge

Sewage sludge is a by-product from wastewater treatment of industrial, municipal or rural sources [17]. The composition of the sewage sludge reflects the use of elements and contaminants in the society [6]. In general, it contains a wide variety of dissolved and suspended impurities and a lot of water (∼99.9 wt%). Examples of impurities in the sewage sludge are organic materials, nutrients, chemical compounds and microbes [18]. The sewage sludge can also contain pollutants such as heavy metals, pharmaceuticals and pathogens [6]. Due to the content of essential plant nutrients, such as P, N and K, sewage sludge is considered to be suitable for recycling of nutrients to agricultural soils [17]. The recycling is done either by spreading the sewage sludge on agricultural soils or by nutrient recovery from incinerated sewage sludge ash. The agricultural use of sewage sludge is restricted by legislation but also influenced by public acceptance, population density and availability of agricultural lands [7].

2.1.3.1 Treatment and disposal of sewage sludge

At the wastewater treatment plant, the sewage sludge is derived from primary, secondary and tertiary treatment processes [17]. The primary treatment is a physical step that commonly includes chemical precipitation and sedimentation, meanwhile the secondary treatment is by biological degradation. The tertiary treatment is an additional processing, that could be required in some processes to improve the removal of impurities. It can include treatments such as effluent polishing of suspended solids and chemical precipitation of plant nutrients [18]. Before final disposal of the sewage sludge, it is desired to reduce the volume by removal of water and stabilise the organic materials to minimise odour and to remove pathogens [17]. Several steps

can be included in the treatment of sewage sludge, but the most commonly applied are thickening, stabilisation and dewatering [18].

Final disposal of sewage sludge is controlled by legislation and commonly applied methods are spreading on agricultural land, incineration or landfilling. Statistics from the European Union showed that in 2018, 50 % of sewage sludge was spread on agriculture soils, 28% was incinerated and 18% was landfilled [7]. Spreading on agricultural land is mainly applied in order to recirculate nutrients and organic matter [17]. The main motivation to incinerate the sludge is to reduce the volume, and thus the cost for transportation [6]. Incineration can further be motivated by legislation that prohibits landfilling in some countries. It is also possible to recover energy from the incineration and nutrients from the sewage sludge ash [7]. Nevertheless, the incineration results in generation of emissions that requires handling with air pollution control systems [15].

2.1.3.2 Spreading of sewage sludge on agricultural land

A commonly applied route for nutrient recovery from sewage sludge is spreading on agricultural land. Most of the countries in the European Union have prohibited direct disposal of untreated sewage sludge on agricultural lands and the most common applications is spreading of treated sewage sludge, called biosolids [7]. The purpose with the treatment is to dewater and stabilise the material and also reduce content of pathogens, as mentioned in 2.1.3.1. Examples of common stabilisation treatments are aerobic digestion, anaerobic digestion, composting and thermal drying [7].

By spreading the sewage sludge on agricultural lands, the plant growth and reproductive success is enhanced. The sewage sludge will function as soil conditioner and fertiliser by supplying the plant with nutrients and organic matter [17]. Furthermore, the spreading on agricultural land improves the physical properties of the soil and reduces the negative effect of losses of organic matter due soil degradation [7]. However, even after treatment, there is still a risk of contamination from the sewage sludge by heavy metals, organic pollutants and pathogens [2]. This has caused a low acceptance to the material in several countries [17]. The contamination also limits its agricultural application due to legislation that controls the content of heavy metals and pathogens in the sewage sludge [7]. Some authors, like Kirchmann et al [6], argues that spreading of sewage sludge is an inefficient recycling method of P. This is mainly due to the high water content and low nutrient concentration in sewage sludge, which makes the transportation expensive and the plant yield low [6].

2.1.3.3 Recovery of phosphorus from sewage sludge ash

Due to the mentioned environmental and health risks related to spreading of sewage sludge on agricultural lands, there is a growing interest to find other methods for recovery of nutrients from sewage sludge [2]. One promising strategy is to recover it from incinerated sewage sludge ash. Since combustion of sewage sludge is estimated to increase as a treatment method, the ash will most likely be a key waste in the future. Thus, the sewage sludge ash will become an available flow for P recovery.

However, since the incineration not only results in enrichment of nutrients, but also of heavy metals, direct application of the ash is most likely not a suitable option. Instead, P should be recovered from the ash and then used as a fertiliser [6]. Today, there exists several methods and techniques, already applied or under development, for extraction of P in various forms from sewage sludge ash [2].

The main motivation to recover P from sewage sludge ash is that the incineration destroys organic pollutants, pharmaceutical residues and pathogens [19]. It is also possible to recirculate P to agricultural soil without a high content of heavy metals [6]. Another important perspective is the high recovery rate of P (60–90% relative to wastewater) [2]. However, during the combustion, the organic matter is destroyed, which possibly could have been used for composting and soil improvement [19]. Also, other nutrients such as N and K are lost during the incineration. N is lost as gas during the combustion and only very small amounts of K is left in the sewage sludge ash after the incineration due to its solubility properties in water. Nevertheless, the losses of N and K could be considered to have little relevance to agriculture due to their low content in the sewage sludge compared to P [6].

2.2 The Ash2Phos process

This section provides a theoretical basis for the investigated process. First, a general overview of the main parts, input and outputs of the process is presented. Thereafter, the separation of Fe, which is the main step of interest, are described in more detail.

2.2.1 General overview

Ash2Phos is a continuous process for P recovery from incinerated sewage sludge ash which consists of several steps at different pH levels. The main parts of the process are acidic treatment, separation of recoverable elements and separation by elements [9]. The main inputs to the process are ash, acid and lime [9]. The main outputs are $Ca_5(PO_4)_3OH$, $FeCl_3$, Al product and silica sand. The most important steps, inputs and outputs of the process are summarised in Figure 2.1.

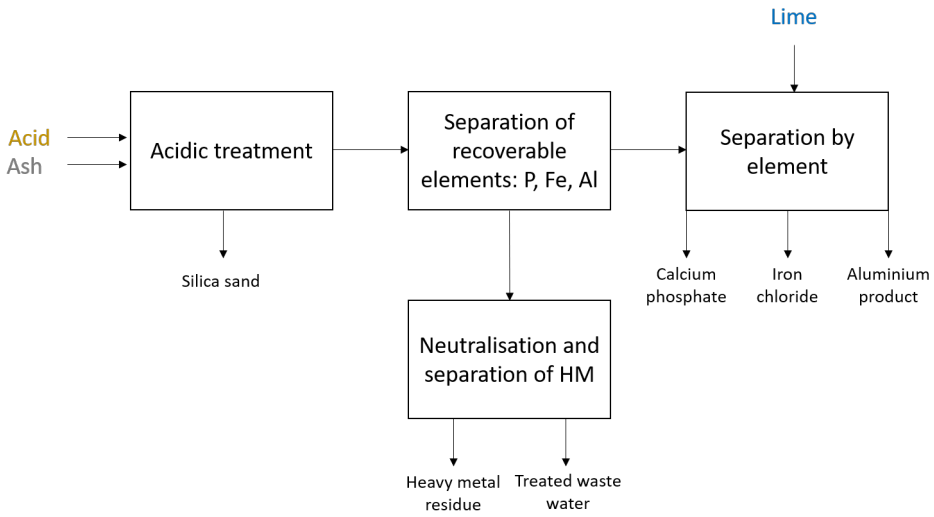

Figure 2.1: *The main process steps in the Ash2Phos process together with the main inputs and outputs.*

As can be seen in Figure 2.1, heavy metals and other unwanted elements are separated from the recoverable elements. The elements of main interest are thereafter treated futher into three different products in several process steps. The wastewater containing harmful substances is also treated in other steps of the process.

2.2.2 Separation of iron

The first separation by element step is the separation of Fe which recovers Fe as a separate stream that can be treated in further steps into the final $FeCl_3$ product. In this step, Fe is separated from P and Al by precipitation in alkaline conditions and filtration, illustrated in Figure 2.2.

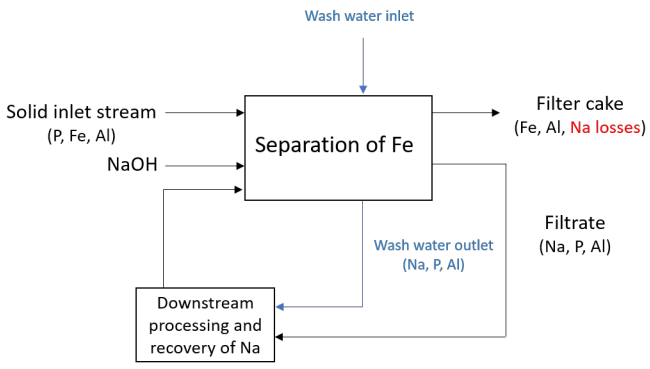

Figure 2.2: *The Fe separation step together with the main components of interest.*

The separation step is further divided into a reactor stage and a filtration stage, described in more detail below. Ideally, all Fe ends up as precipitate in the filter cake while all Na and P are kept dissolved and ends up in the filtrate. However, during the development of the process, undesired losses of Na to the filter cake have

been discovered. A reduction of these losses is desirable in order to increase resource efficiency and reduce the operational cost related to the process step.

2.2.2.1 The reactor stage

The first stage of the Fe separation consists of a reactor which is fed with the stream containing P, Fe and Al after removal of unwanted compounds. NaOH and recirculated streams from downstream processing containing recovered Na are also added and a slurry is created by mixing. The main purpose of the reactor stage is to trigger the precipitation of Fe and the dissolution of P by increasing the pH. However, other unwanted precipitates, possibly including Na, can simultaneously form in the reactor due to the pH adjustment and addition of chemicals.

2.2.2.2 The filtration stage

In the filtration stage, the slurry from the reactor stage is filtered with vacuum and the filter cake is washed on the filter bed with water. The filter cake is thereafter directed for further processing and the filtrate is directed to the production of P and Al products, according to Figure 2.2. After downstream processing, the liquid streams are recycled back to the reactor in order to recycle NaOH and reduce the need for expensive NaOH make-up. The dominating component in the filter cake is Fe-precipitate but significant amounts of Al-silicates enter the reactor with the solid inlet stream and follows to the filter cake. These silicates are interesting to investigate since a variety of silicates have been proven to have suitable properties for adsorption of metals in aqueous solutions [20],[21],[22],[23],[24] which is known to be one mechanism responsible for material losses in filtration processes [10].

2.3 Precipitation and dissolution reactions theory

The reaction stage in the separation of Fe is based on precipitation of Fe and dissolution of P by addition of NaOH. This is an example of precipitation and dissolution reactions which utilises the change in solubility of different compounds at varying conditions. These reactions are commonly used in P recovery processes that has been under development but can also be found in wastewater treatment [8],[25],[26]. This sections provides the theory of solubility in general as well as a small summary of the utilisation of precipitation and dissolution in P recovery from sewage sludge ash.

2.3.1 Solubility

The solubility of a solid compound in a liquid phase depends on pH, competing ions and temperature [25],[26],[27]. It describes the maximum concentration of a compound that can be dissolved under the specific conditions and can be expressed in terms of g solute/mL of used solvent [28].

2.3.1.1 The solubility product

There is always an equilibrium between the solid phase and the dissolved ions of the same substance in a saturated solution [29]. The equilibrium constant of a dissolution reaction is also known as the solubility product, K_{s0} [27]. For the general dissolution equilibrium reaction between the solid consisting of species A and B, shown in equation (2.1),

$$A_a B_b(s) \leftrightarrow aA^{m+} + bB^{n-} \tag{2.1}$$

the solubility product is expressed according to equation (2.2),

$$K_{s0} = \gamma_A^a \gamma_B^b [A^{m+}]^a [B^{n-}]^b \tag{2.2}$$

where γ_A is the activity coefficient for A and γ_B is the activity coefficient for B [27]. If the right term in equation (2.2) is larger than the left term, precipitation of the solid phase will occur until the terms are equal. If the right term is smaller, the solid phase will instead dissolve until the equilibrium has been reached.

2.3.1.2 Precipitation by addition of a common ion

The solubility of a certain substance in solution can be decreased by addition of a common ion which forms a precipitate with the substance of interest. One example is enhanced precipitation of heavy metals in wastewater by addition on excess hydroxide ions [29]. Due to the ion addition, the system will counteract the hydroxide excess in the solution by precipitation of heavy metal hydroxides.

2.3.2 Precipitation and dissolution in phosphorus recovery

Heavy metals and other unwanted elements present in the sewage sludge ash need to be removed from the P to limit the content of hazardous substances and to increase the quality of the final product [30]. Several P recovery methods based on selective precipitation and dissolution of compounds from incinerated sewage sludge ash have been investigated [8],[25],[31].

The P in incinerated sewage sludge ash is often present as phosphates of Ca, Fe or Al. Some processes are based on acid leaching at pH < 2 in which these P compounds are completely dissolved [30]. One problem with this approach is that most of the heavy metals are left in the dissolved phase after the treatment as well, and need to be separated from the P. It is also desirable to separate the dissolved Al and Fe from P in order to improve the quality of the product. Both these issues creates a demand for further separation steps after the acid leaching [8],[25]. Ion-exchange, solvent extraction and precipitation are some examples of methods that have been suggested as possible solutions.

Other proposed processes uses only alkaline leaching of the incinerated sewage sludge ash [30],[31]. In this approach, only the Al-phosphates dissolve completely and heavy metals are directly separated as solids from the P. The efficiency of this method is, however, dependent on the content of Ca and Al in the ash [30].

Further studies have investigated combinations of both acidic and alkaline treatments by triggering the precipitation of different compounds in several steps resulting in an efficient P recovery and a high quality product free from heavy metals [8],[25].

2.4 Filtration theory

Filtration is used in the separation of Fe to separate the solid Fe-precipitate from the dissolved P. Filtration is a commonly used unit operation in which mother liquor and solids in a slurry are separated into a filter cake and a filtrate. The process can be conducted as a batch process or as a continuous process and several driving forces such as pressure or vacuum can be used [10]. To improve the efficiency of the separation and increase the purity of the filter cake, it is common to use a washing step for further removal of undesired elements [32]. However, several properties of the filter cake have an effect on the efficiency of the filtration and washing processes. This section provides the main theoretical concepts of filtration and washing and possible causes of material losses in such processes.

2.4.1 Washing of filter cakes

There are two main types of particle washing procedures which can be conducted separately or in combination, either in co-current or counter-current mode [10],[32]. The first type is dilution washing in which a filter cake is resuspended in the wash liquid to a slurry which is separated in the next step. This sequence is thereafter repeated several times until the desired purity of the solid has been reached. The second type is only applicable in filter cake washing and is hence the main focus in this section. This type is called permeation washing. In this procedure, mother liquor in the filter cake is displaced with washing liquid on a fixed bed directly after the filtration [33]. This introduces characteristic fixed particle-particle and particle-wall interactions that cannot be targeted in the same way as in dilution washing [33]. Two mechanisms are involved in permeation washing. These are displacement and diffusion [32]. The phenomena observed during the permeation washing process can be represented by a washing curve describing the relationship between amount of impurities left in the filter cake and the amount of wash liquid used. A straight forward way to express this is to use the concentration ratio, C^*, based on the liquid analysis of filtrate and wash liquid and the wash liquid ratio, W, [10],[33]. C^* is expressed as the ratio between the impurity concentration in the wash liquid (or filtrate) after each wash, C [M], and the impurity concentration in the filtrate, C_0 [M], expressed in equation (2.3) [10].

$$C^* = \frac{C}{C_0} \tag{2.3}$$

The wash liquid ratio is the ratio between the mass of wash liquid added, m_{WL} [kg], or volume [L], and the mass of mother liquor, or volume, in the filter cake, m_{ML} [kg], presented in equation (2.4) [10].

$$W = \frac{m_{WL}}{m_{ML}} \tag{2.4}$$

However, the most accurate results are obtained by knowing the exact concentration in the filter cake from the start and after each wash [32]. The concentration in the outlet wash liquid can be related to the amount of impurities in the filter cake by using the impurities loading, X. The loading is defined as the ratio between the mass of dissolved and adsorbed impurities in the filter cake, (m_{sol}+m_{ads}) [kg], and the total mass of the filter cake, m_s [kg], expressed in equation (2.5) [10].

$$X = \frac{m_{sol} + m_{ads}}{m_s} \tag{2.5}$$

The loading can thereafter be expressed in terms of the loading ratio, X^*, between the current loading, X, and the initial loading, X_0, according to equation (2.6) [10].

$$X^* = \frac{X}{X_0} \tag{2.6}$$

Furthermore, the loading ratio can also be expressed according to equation (2.7) [10].

$$X^* = 1 - \int_{W=0}^{W} C^*(W)\Delta W \tag{2.7}$$

The relation between X^* and W or the relation between C^* and W can be plotted after data have been collected in a washing experiment. It can, however, be noted that the resulting plots in most cases can be considered to follow the same behaviour [10]. In the ideal case, only one washing step using one bed volume of wash liquid would be needed to reduce the impurities completely. However, this is generally not the case in real washing processes. Instead, a real washing curve has three main segments [32],[33]. A typical washing curve using C^* as well as the ideal case is represented in Figure 2.3.

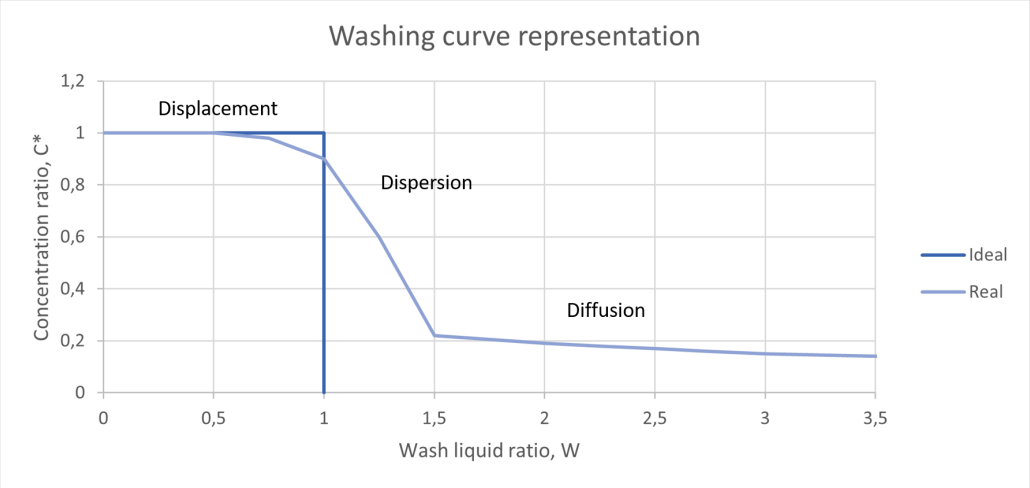

Figure 2.3: *A representation of an ideal and a real washing curve during permeation washing [10],[32],[33]. The three different regimes with the dominating mechanisms are also marked in the figure.*

.

Only in the first segment, the typical curve resembles the ideal curve quite well and the main mechanism here is displacement, as can be seen in Figure 2.3 [10],[33]. In practice, this means that pure mother liquor is obtained during the wash. Thereafter, the dispersion region is reached. In this region, wash liquid and mother liquor are undesirably mixed, which results in a deviation from the ideal behaviour. In the last region, diffusion is the limiting factor and the washing continues more slowly until an adsorption equilibrium has been reached [32].

2.4.2 Filter cake properties and limitations

A filter cake has several properties that can influences the filtration and the washing procedures [34]. One of the most important aspect is the porosity of the cake, where the porosity itself also depends on other variables such as particle size distribution, particle shape and cake formation conditions [35]. Some important aspects of particle sizes, pore sizes and other limitations are summarised below.

2.4.2.1 Particle size distribution

The size of the particles is an important variable not only due to its effect on the porosity, but also because small particles tend to form cakes of high resistance that are more difficult to wash [36]. In such cases, it is possible to add a filter aid that facilitates the filtration and washing processes [34]. If the particles are very porous, on the other hand, smaller particles can be easier to wash since diffusion from the inner pores of small particles are faster than from larger particles [10].

2.4.2.2 Pore size distribution

The pore size distribution in a filter cake has a significant effect on the washing efficiency [32],[35]. The reason is that a large variety of pore sizes results in a large variety of flow rates through the different pore sizes which makes the flow deviate more from an ideal plug flow. In turn, a less ideal flow of wash liquid increases the washing time and the amount of wash liquid that will be needed to obtain the correct purity of the filter cake. Another aspect of the porosity is that smaller pores give more narrow channels in the cake. This results in a larger flow resistance which in turn leads to a slower displacement process [33]. The surface charge and thus the pH (among other variables) can affect the cake porosity and the flow resistance in a filter cake, and thus also the filtration and washing [34].

2.4.2.3 Limitations of filtration and washing

It is not always possible to remove all undesired elements by filtration and washing, even with large amounts of wash liquid added. Impurities trapped in the filter cake after the washing can for instance be found in isolated pores, in the small space between particles or adsorbed onto the particle or pore surfaces which makes the mother liquor inaccessible for the wash liquid [10],[33]. A representation of different areas that can be responsible for undesired impurities in a filter cake is displayed in Figure 2.4.

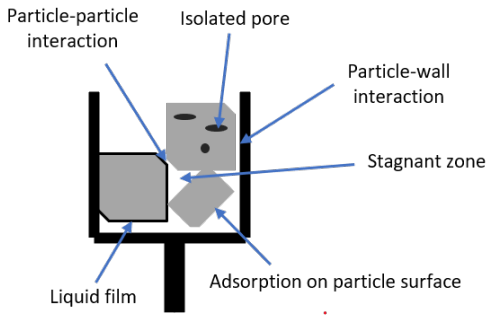

Figure 2.4: *Examples of areas that are problematic to reach during washing [10].*

From these hidden areas impurities can, for instance, be removed by adjusting pH and temperature to affect the adsorption equilibrium concentration, by resuspension of the cake (as in dilution washing) or by total dissolution of the particles [10],[32],[33]. Several technical limitations can also be added to the list but this will not be mentioned further [32].

2.5 Adsorption theory

Adsorption is a surface phenomenon where the adsorbate from the bulk fluid are adsorbed onto the solid adsorbent surface [37]. Adsorption is commonly divided into chemisorption and physisorption, based on interaction strength. Chemisorption occurs due to formation of covalent bonds between the adsorbate in the solution

and the substrate on the solid surface. The adsorbed molecules form a monolayer onto the adsorbent. Physisorption occurs due to the weak electrostatic interactions where the adsorbate forms a multilayer on the adsorbent surface [38]. Adsorption processes are commonly applied for separation and purification, both in gas and liquid mixtures [37]. This sections provides the theory of adsorption in aquatic systems, adsorption equilibrium and the construction of adsorption isotherms.

2.5.1 Adsorption in aquatic systems

Adsorption in aquatic systems can be seen as accumulation of substances at the solid-liquid interface. It can influence the reactivity and the electrostatic properties of the solid surfaces as well as the distribution of substances between the aqueous and solid phase [39]. Adsorption reactions at solid surfaces consists of both chemical bonds between the solutes and the surface atoms as well as electrostatic interaction between ions and charged surfaces [40]. The rate of adsorption in aquatic systems is controlled by accessibility of the surfaces to the ions in the solution [22]. This means that the particle size distribution is an important factor for surface adsorption, since it affects the surface area available for adsorption [40]. Thus, the smaller particles, the larger total surface area. For porous systems, the rate is also controlled by the rate of ion diffusion, which then is related to the size and shape of the pores inside the particles [22].

In aquatic systems with oxides of Si, Al, Fe and Mn, metal ions and ligands can be adsorbed on the oxide surface [40]. The adsorption of cations on the surface is typically a very rapid process [22]. Surface complex formation with metals involves both coordination of the metal ion in the solution as well as coordination of the proton in the OH-group at the metal oxide surface. The metal complexes can be formed either as inner-sphere or outer-sphere complexes. An inner-sphere complex is formed by covalent bonding between the metal ion and the oxygen at the surface ligand. An outer-sphere complex is formed by ion pairing with H_2O between the surface ligand and the metal ion. The main differences between them are that outer-sphere complexes are highly dependent on ionic strength, which involves electrostatic bonding and are therefore less stable compared to inner-sphere complexes. The latter on the other hand, typically involve covalent and/or ionic bonding, which results in a higher stability [39]. Surface complex formation with ligands occurs mainly through ligand exchange between a surface ligand and a solute ligand at the metal ion of the oxide surface. They can also be formed as either inner or outer-sphere complexes [39].

The tendency for adsorption on oxide surfaces depends on the affinity of the surface sites for metal ions or ligands and the activity of the surface sites, which is dependent on pH [39]. For ions of alkali and earth alkali metals, the adsorption affinity is increasing with the ionic radius of the ion, as illustrated in equation (2.8) and (2.9), respectively [39].

$$Li^+ < Na^+ < K^+ < Rb^+ < Cs^+ \tag{2.8}$$

$$Mg^+ < Ca^+ < Sr^+ < Ba^+ \tag{2.9}$$

In general, the adsorption onto oxide surfaces is highly dependent on pH, and both the binding of metals and ligands on oxides surfaces varies with pH [39]. The adsorption of metal ions on an oxide surface is favoured by higher pH, due to decreased competition between H^+ and surface ligands [40]. For adsorption of ligands, the opposite applies since the adsorption is coupled to release of OH^- [39]. However, it is also of great importance to notice that each metal and ligand has its specific pH range, where it adsorbs on oxides surfaces.

2.5.2 Adsorption isotherms

In order to understand adsorption processes, information about the adsorption equilibrium is crucial. Equilibrium performance of an adsorption process depends on type of adsorbate and adsorbent as well as of various physical properties of the solution, such as pH, ionic strength and temperature [38]. A common method to describe the adsorption equilibrium is to use adsorption isotherms that relate the concentration of adsorbate in the solution with the amount adsorbed onto the surface at a constant temperature [39]. Adsorption isotherms can also give information about the interaction mechanisms between the adsorbate and the adsorbent [38]. The adsorption isotherms are considered to be fundamental tools to model and illustrate adsorption systems and several models have been developed. The most commonly applied optimum isotherms in adsorption studies are the Langmuir model and the Freundlich model. The main reason is related to the simplicity of applying these methods by linear regression [37].

2.5.2.1 The Langmuir model

The Langmuir model is the most frequently used model for adsorption in solutions [22]. It is a chemical isotherm model based on four basic assumptions [37]. First of all, it considers monolayer adsorption where the adsorbate molecules are adsorbed at adsorption sites of the adsorbent. Secondly, the distribution of adsorption sites is assumed to be homogeneous. Thereafter, the adsorption energy is assumed to be constant and finally, the interaction between the adsorbate molecules is assumed to be negligible. There exist both a linear and nonlinear Langmuir model, illustrated by equation (2.10) and equation (2.11), respectively [22],

$$\frac{C_e}{Q_e} = \frac{1}{Q_m K_L} + \frac{C_e}{Q_m} \tag{2.10}$$

$$Q_e = \frac{Q_m K_L C_e}{1 + K_L C_e} \tag{2.11}$$

where Q_m is the maximum adsorption capacity [mol/g], Q_e is the equilibrium metal ion concentration on the adsorbent [mol/g], C_e is the equilibrium metal ion concentration in the solution [mol/L]and K_L is the Langmuir adsorption constant [L/mol].

2.5.2.2 The Freundlich model

The Freundlich model is an empirical model that lacks physical meaning [37]. The Freundlich adsorption isotherm describes a reversible and non-ideal adsorption pro-

cess and it can be applied for multilayer adsorption on heterogeneous surfaces [38]. There exist both a linear and nonlinear Freundlich isotherm, illustrated in equation (2.12) and equation (2.13) [22],

$$\ln Q_e = \ln K_F + \frac{1}{n} \ln C_e \tag{2.12}$$

$$Q_e = K_F C_e^{1/n} \tag{2.13}$$

where K_F is an empirical constant related to the adsorption capacity and n is an empirical constant related to the adsorption intensity.

3
Methods

The first part of this chapter provides the theoretical background to the analytical techniques applied. Thereafter, the conducted experimental procedure will be described. Finally, the sample analysis procedures that were not externally analysed will be presented.

3.1 Analytical techniques

This section gives a theoretical basis for the analytical techniques that are used for the liquid and solid analyses described in section 3.2.

3.1.1 Spectrophotometry

Spectrophotometry is an analytical technique that uses light of different wavelengths, such as UV-light, to determine the concentration of one specific compound in a sample [41]. The spectrophotometer usually consists of a radiation source, a monochromator, a sample cell and a detector and a schematic overview of a typical setup is illustrated in Figure 3.1.

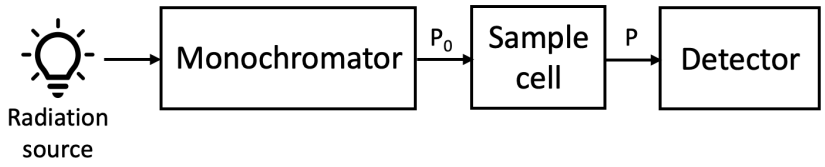

Figure 3.1: *Schematic overview of spectrophotometer setup where P_0 is the starting irradiance and P is the the irradiance of the light after passing the sample cell [41].*

When the light is emitted from the light source, it passes through the monochromator in which one wavelength is being selected. After the monochromator, the monochomatic light passes through the sample with the starting irradiance, P_0 [energy/second/unit area of the light beam]. If the light has been absorbed by the sample, the irradiance of the light after passing the sample, P [energy/second/unit area of the light beam], which is measured in the detector, will be smaller than P_0. The absorbance, A, correlates to the change in irradiance according to equation (3.1),

$$A = log(\frac{P_0}{P}) = -logT \tag{3.1}$$

where the ratio between P_0 and P, T, is the transmittance [41]. The absorbance can thereafter be converted into a corresponding concentration according to the Beer-Lambert law presented in equation (3.2),

$$A = \varepsilon cl \tag{3.2}$$

where ε is the molar absorbtivity $[M^{-1}cm^{-1}]$, c is the molar concentration [M] and l is the optical length [cm] [41]. Since many light-absorbing compounds can be present in the sample, it is important to measure the absorbance of a wavelength that distinguishes the compound of interest from others present in the sample [41]. Furthermore, the measurement should be done at the wavelength corresponding to the maximum absorbance.

3.1.1.1 LCK cuvettes for analysis of iron, aluminium and phosphorus

In some applications, LCK cuvettes from Hach Lange can be used for a quick spectrophotometrical analysis. The main idea is to use cuvettes that are pre-filled with reagents that can form a compound with a target ion in a sample when it is added according to the corresponding method for each individual element [42],[43],[44].

For the Fe determination, ascorbic acid must first be added to reduce all Fe(III) to Fe(II). The Fe(II) ions can thereafter form a orange-red complex with 1.10-phenanthroline present in the LCK321-cuvette within 15 minutes [42]. For the Al determination, a weakly acidic acetate-buffered solution must be added to the cuvette prior to the analysis [43]. When the sample is added, chromazurol S present in the LCK301-cuvette can form a green colored lake with the Al present in the sample within 25 minutes. Finally, for the P determination, the diluted sample can be directly added. Phosphate ions in the sample can thereafter form a yellow dye with vanadate-molybdate reagent present in the LCK040-cuvette within 10 minutes [44]. However, this type of analysis is only valid within a certain pH and concentration range. The LCK cuvette number as well as the limitations of each method for Fe, Al and P are summarised in Table 3.1.

Table 3.1: *Summary of the Hach Lange methods for Fe, Al and P [42],[43],[44].*

Element	LCK cuvette	pH range	Concentration range
Fe	LCK321	3-10	0.2-6.0 mg/L Fe
Al	LCK301	2.3-3.5	0.02-0.5 mg/L Al
P	LCK040	3-10	1.6-30.0 mg/L PO_4-P

The accuracy of each method can only be assured when the measurement is within the ranges presented above. Due to the sensitivity of the cuvettes, samples can only be measured within a certain concentration limit and elements of low concentraton cannot be analysed. To obtain a more accurate and complete result of a sample containing many elements, the analysis should therefore be combined with another method such as ICP-AES.

3.1.2 Inductively coupled plasma-atomic emission spectroscopy

Inductively coupled plasma-atomic emission spectroscopy (ICP-AES) is an analytical method, which is used to measure the concentrations of chemical elements in a liquid sample by decomposing it to atoms and ions in a plasma and measure the atomic emission spectra [45]. Since all chemical elements will generate emissions simultaneously, it is possible to both do rapid sequential analysis as well as simultaneous multi element analysis [46].

An ICP-AES consists of two parts, an inductively coupled plasma part and an optical emission spectrometer unit that detects the emissions [47]. The plasma can be described as a flowing stream of hot gas, commonly Ar [46]. It is generated by partially ionising the gas by a spark from a tesla coil in a ICP burner. Due to a high radio-frequency field, the free electrons are accelerated and the energy is transferred to the entire gas by collisions between the free electrons and atoms. The main strength of the ICP is the stable and high operating temperature, that typically can be between 6000-10000 K [45]. A schematic overview of a typical ICP-AES setup is illustrated in Figure 3.2.

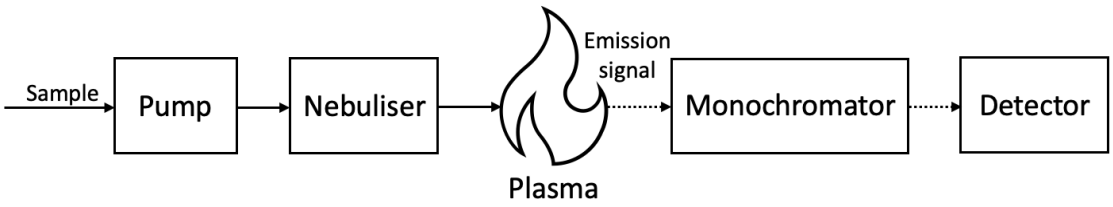

Figure 3.2: *Schematic overview of an ICP-AES setup [45].*

The sample of interest is commonly added to the plasma as an aerosol of small droplets by a nebuliser [47]. As the droplets of sample enters the plasma, they are desolvated and vaporised at the high temperature and later also atomised and ionised [48]. Inside the plasma, collisions between chemical elements and the gas will occur, which causes a part of the atoms and ions to be excited. As the electrons deexcites back to a lower energy state, they will emit photons [45]. The emissions generated are separated in a monochromator based on wavelengths [41] and measured by a detector, commonly a photomultiplier or charge coupled device (CCD) [45]. Since the emission intensity is proportional to the concentration of specific elements, it can be used to both identify and quantity the elements in the analysed sample. The detection limit for ICP-AES is typically around 0.1–10 ng/g for most chemical elements [45].

3.1.3 Inductively coupled plasma-mass spectrometry

Inductively coupled plasma-mass spectrometry (ICP-MS) is an analytical method to determine composition and quantify chemical elements of a liquid sample [49]. It operates using many of the principles of ICP-AES, described in section 3.1.2. The major difference is the detection method, which instead measures the ionised elements in the plasma according to the mass-to-charge ratio [45]. In the mass

spectrometer, the ions in the plasma are separated according to their mass-to-charge ratio with a mass analyser, commonly a quadrupole or magnetic sector. Further, the separated ions are measured by a detector, which typically is an electron multiplier [48]. As with ICP-AES, ICP-MS can be used to both identify and quantify the sample composition. It is possible to detect all elements at once and the detection limit is very low, typically between 0.00001-0.0001 ng/g [45]. Examples of important factors that affect the detection limit are type of element, sample matrix, dilution factor, equipment set-up and instrument operating conditions [48].

3.1.4 Scanning electron microscopy

A scanning electron microscope (SEM) is a type of electron microscope and it can be applied to study surfaces of dry solid objects [50]. It can both be used to image sample surfaces and to analyse bulk samples [51]. SEM utilises a beam of focused electrons in vacuum as an electron probe of relatively low energy to scan over the sample [50]. The electron beam is generated by an electron gun and it is converged into a fine and focused beam by electromagnetic lenses [52]. It is the the interaction between the sample surface and the electron beam that results in emissions of low-energy secondary electrons, high-energy backscattered electrons, Auger electrons and characteristic X-rays [51]. However, it is mainly secondary electrons as well as backscattered electrons that are utilised in SEM for generation of images of the sample. The secondary electrons are produced close to the sample surface through inelastic collision with valence electrons of the atoms [53]. By detecting these secondary electrons, an image of the topographical structure can be generated [52]. The number of secondary electrons detected is affected by the inclination of the sample surface [51]. The backscattered electrons are produced through elastic collision with the nucleus of the sample atoms [53]. They can be detected and used to produce an image of the compositional distribution of atoms at the surface. Number of backscattered electrons reflected are dependent on the composition, atomic number and crystal orientation of the atoms [52].

3.1.4.1 Energy dispersive spectrometry

An elemental analysis of the sample can be accomplished by combining the SEM with a detector that can detect emitted X-rays [52]. The X-ray signals can be utilised for chemical identification of atoms on the sample surface [53]. A commonly applied technique is to use an energy dispersive spectrometer (EDS), which measures the energy of the characteristic X-rays from the number of electron-hole pairs generated [54]. Since each chemical element is related to a particular wavelength, it is possible to both detect and quantify elements in the sample [52]. The detection limit for elements with EDS is in general 0.1 wt%. This means that it is possible to track major and minor elements, meanwhile trace elements will not be detected. Another important factor for the detection in EDS is the surface condition of the sample. Thus, a smoother surface will give a lower detection limit [53].

3.1.5 X-Ray powder diffraction

X-ray powder diffraction (XRD) is used to detect crystalline structures and to determine their relative amount in a sample [55]. The very specific and structured organisation of atoms and molecules in a crystalline material, as well as the size of the distance between them, make it possible to use an X-ray beam to distinguish one structure from another [55]. The analysis and the determination of the crystal structure is based on the Bragg equation shown in equation (3.3),

$$n\lambda = 2dsin\theta \tag{3.3}$$

where n is an integer, λ is the wavelength of the electrons, d is the spacing of crystal planes and θ is the angle of incidence [56]. The concepts are further represented in Figure 3.3.

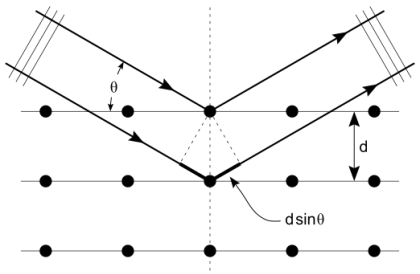

Figure 3.3: *Definition of the spacing between the crystal planes as well as the angle of incidence in the Bragg equation from [57], CC-BY-SA 3.0.*

Before the analysis, wet samples need to be dried and coarse samples need to be milled into a fine powder. The sample is pressed into a holder to even the surface and is thereafter placed in the sample chamber. Often, only one specific X-ray wavelength are allowed to reach the sample [55]. The X-rays are created in an X-ray tube with a heated tungsten filament that are supplying electrons to another metal, often copper, in vacuum [55],[58]. The resulting energy loss after the collision is released as X-rays. During the measurement, the X-ray beam is directed towards the sample which is scanned and simultaneously rotated using a goniometer [55]. When the beam hits the sample from a variety of angles, energy will be emitted resulting in an X-ray pattern with peaks of different intensities at specific 2θ-values. The spectra can thereafter be matched to certain structures from a database since each specific set of peaks, with respect to size and location, corresponds to a specific chemical composition and crystal structure. The detection limit for XRD is typically around 1% [55].

3.2 Experimental procedure

This section describes the practical aspects of the investigation which involved laboratory experiments on semi-pilot scale and on lab scale.

3.2.1 Process reproduction on semi-pilot scale

The process reproduction experiment was designed to investigate the cause of Na losses during separation of Fe as well as the influence of wash water ratio on the filter cake composition. The process was, however, simplified and only performed on a semi-pilot scale. The large scale process is continuous while the process steps in these experiments were performed in batches. To create a representative simulation of the process and bring the system to a certain equilibrium, some steps had to be performed in several cycles. The first process step, ash leaching, was for simplicity only conducted in one batch. The following steps, separation of recoverable elements (P, Al, Fe) and separation of Fe, were on the other hand performed in cycles. Further, since the focus of the experiment was to investigate the Fe separation step, downstream steps were not performed. However, the large scale process involves several recirculations from downstream steps that have an effect on the steady state composition of the process streams. Therefore, some artificial solutions, representative for recirculated streams, were prepared.

The down-scaling from large scale to semi-pilot scale was based on using 1 kg of the ash leaching solution in the first process step into each cycle. Ratios between varying process streams from the large scale process were thereafter used to recalculate all streams. Further, all process steps conducted during the semi-pilot scale experiment involved filtration followed by washing of the formed filter cake with fresh tap water. The wash water amount needed after filtration in the ash leaching (section 3.2.1.2) and the cycles (section 3.2.1.3 and 3.2.1.4) were calculated before the washing of each cake was performed. The mass of wash water needed for the filter cake or cycle i, $m_{ww,i}$ [kg], was calculated based on the dry solids (DS) [%] measurement from the previous cycle according to equation (3.4),

$$m_{ww,i} = W_{m,i} \cdot m_{wet,f,i} \cdot (1 - DS_{(i-1)}) \tag{3.4}$$

where $W_{m,i}$ is the desired wash water ratio and $m_{wet,f,i}$ [kg] is the mass of the cake after filtration, but before the washing. For the ash leaching and for the first filter cake produced in the first step of the cycles, the value was approximated based on the large scale process. To avoid cracks in the cake, the washing of each cake was started when the mother liquor reached the surface of the filter cake, meaning that the DS of the cake was slightly lower compared to the cake after washing, after which all accessible water has been removed. After finishing the cycles, the real wash water ratio, $W_{m,real,i}$, was calculated for each cycle based on the correct DS, wet cake mass after washing, $m_{wet,w,i}$ [kg] and the mass of wash water added according to equation (3.5).

$$W_{m,real,i} = \frac{m_{ww,i}}{m_{wet,w,i} \cdot (1 - DS_i)} \tag{3.5}$$

The correct values of the wash water ratio were thereafter used together with the results from the ICP-AES analysis of the outlet streams of the Fe separation step to evaluate the washing performance of the filter cake. The following sections will provide a more detailed description of the preparation of artificial solutions, the ash leaching in batch and the following cycles that were performed with and without addition of artificial alkaline solution.

3.2.1.1 Preparation of acidic and alkaline artificial solutions

One acidic solution was mixed in order to mimic inlet streams to the acidic part of the process. To this solution, $NaAlO_2$ (s), $CaCl_2 \cdot 2H_2O$ (s), NaOH (50%), H_3PO_4 (85%), $FeCl_3$ (40%) and tap water were added aiming at concentrations similar to the recirculated streams of the large scale process to a total volume of 10 L. To assure complete dissolution, solid chemicals were pre-dissolved with heating before adding the additional water. Unfortunately, unknown precipitate was found in the canister after one night. Therefore, the acidic solution was exchanged by tap water and by adding some acidic streams from previous cycles.

One alkaline solution was also prepared as a representation of recirculated streams to the Fe separation step. During the first attempt, $NaAlO_2$ (s), NaOH (50%), H_3PO_4 (85%) were mixed with tap water to representative concentrations and a total volume of 21 L. Again, solid chemicals were pre-dissolved before additional water was added. However, precipitate was noticed in this canister as well after one night. A second attempt was performed by exchanging the tap water with demineralised water. In this canister, no significant precipitation was discovered and the solution was used as an input to the cycles described in section 3.2.1.3.

3.2.1.2 Ash leaching

The ash leaching was performed in one batch prior to the reaction cycles to produce acidic filtrate and acidic wash water needed as input for all cycles at once. The leaching was performed in a 30 L reactor and the rector was equipped with baffles and the stirring was performed by a overhead mixer. The first step was to add tap water to the reactor. In the second step, the ash was slowly added during stirring and in the last step, addition of HCl solution (37%) was performed. The slurry was made based on a certain ratio of water to ash as well as a certain ratio of acid to ash, which both corresponds to optimised values from the large scale process.

After the reaction time had passed, the temperature was measured and the slurry was filtered. Initially, the slurry was supposed to be dosed into a Büchner funnel for vacuum filtration using Munktell filter paper (class 00M). However, due to blockage of the filter and extremely low filtration rate, the filtration was performed on a pilot scale Larox press filter with a filter area of 0.1 m^2. The wash water amount used was based on a wash water ratio of 1.5. Both filtrate and wash water was collected and used in the upcoming cycles.

3.2.1.3 Cycles with artificial alkaline solution

Two process steps, separation of recoverable elements and separation of Fe, were mimicked in several cycles on a semi-pilot scale. This was performed by using artificial alkaline solution to mimic recirculations from downstream steps until an unwanted accumulation of Al in the filter cake was discovered after three cycles.

3.2.1.3.1 Separation of recoverable elements

In the separation of recoverable elements an initiation step (cycle 0) was needed in which no recirculations were done and fresh chemicals of required amounts were added to initiate the system. For all cycles, liquid from the ash leaching was mixed with other recirculated streams in a 2.5 L reactor with overhead mixing. The pH was adjusted to trigger precipitation of Fe, Al and P compounds and was thereafter continuously measured during the reaction. Thereafter, the temperature of the slurry was noted and the solid and liquid phases were separated with vacuum filtration on a Büchner funnel using Munktell filter paper (class 00M). The filter cake was thereafter washed using a cylinder with tap water at 55-57 ℃ with a target wash water ratio of 1.5. After each step, concentrations of P, Al and Fe in the liquid phases were spectrophotometrically analysed with Hach Lange + LCK cuvettes in order to estimate the reaction progress in each cycle (section 3.3.1). In addition, the pH of the filtrate and wash water were checked. The solid phase was weighted and analysed for DS. Some of the streams were also collected and used as input to the next cycle.

3.2.1.3.2 Separation of iron

In the separation of Fe, the solid phase from the previous step was mixed with tap water, artificial alkaline solution and other recirculated streams in a 5 L reactor with overhead mixing. NaOH-solution was thereafter added to increase the pH to the desired value to trigger the formation of Fe-precipitate and the dissolution of P. The pH was also continuously checked during the reaction. The formed slurry was thereafter filtered on a Büchner funnel using Munktell filter paper (class 00M) and washed using a cylinder with tap water at 55-57 ℃ using a target wash water ratio of 1.5. After each step, concentrations of P, Al and Fe in the liquid phases were analysed spectrophotometrically with Hach Lange + LCK cuvettes to establish mass balances and track the reaction progress in each cycle. The mass of the solid phase was noted and the cake was analysed for DS. Liquid streams were collected for recirculation and the volume and weight of the streams were noted. The pH of the resulting filtrate and wash water was also checked.

During the tracking of concentrations, an undesired accumulation of Al in the cake was, however, discovered after cycle 3. This was most likely due to precipitation of an Al compound from one of the chemicals used in the artificial alkaline solution. Therefore, the procedure had to be restarted by exchanging the artificial solution with tap water (section 3.2.1.4). A part of the filter cake from the last cycle was

however still dried in an oven at around 115 ℃ and saved for analysis with SEM-EDS and XRD and another was sent for external dissolution and analysis with ICP-MS.

3.2.1.4 Cycles without artificial alkaline solution

To produce a filter cake without undesired Al precipitate, the alkaline artificial solution was exchanged by tap water. Furthermore, precipitate was discovered in both filtrate and wash water from the ash leaching before the initiation cycle was started. This precipitate was filtered off and the remaining filtrates were analysed with HACH Lange + LCK cuvettes for P, Al and Fe. Since the concentrations of major elements were still within the acceptable range according to desirable compositions from the large scale process, the filtered solutions were used as liquid inlet streams in the following cycles, however with some losses of elements that should be present in the large scale process.

By using tap water instead of the artificial alkaline solution, the total liquid volume into the reactor was kept equal. The cycles were performed until a near-equilibrium was reached resulting in a total of six cycles. In these cycles, some additional exceptions compared to the first run of cycles (section 3.2.1.3) were also added. Since the time for experiments were limited, only the P concentration was tracked in the filtrate with Hach Lange + LCK cuvettes. Instead, all filtrate and wash water streams were diluted with demineralised water and sent for external macro elemental analysis with ICP-AES. Solid streams were collected and sent for external dissolution and analysis with ICP-MS.

3.2.1.4.1 Separation of recoverable elements

The separation of recoverable elements was performed in the same way as mentioned in section 3.2.1.3. In the end of cycle 4, an extra sample of the solid outlet was collected, dried in an oven at around 115 ℃ and saved for solid sample analysis with SEM-EDS and XRD. Finally, the target wash water ratio was increased to 2.5 starting from the first cycle in order to get a better wash of the cake.

3.2.1.4.2 Separation of iron

Besides from exchanging the artificial alkaline solution with clean tap water, the Fe separation step was conducted with the same procedure as described in section 3.2.1.3 but with some exceptions. The target wash water ratio was increased to 2.5 starting from the first cycle in order to get a better wash of the cake. During the third cycle, the DS of the slurry was adjusted by decreasing the addition of liquid streams aiming at the known steady state value from the large scale process. This was repeated for the rest of the cycles.

After the fifth cycle, an additional sample of the filter cake was dried in an oven at around 115 ℃ and saved for analysis with SEM-EDS and XRD. This filter cake was assumed to be near steady state and therefore saved as the sample for the conditions which will be referred to as normal washing (target wash water ratio 2.5). Furthermore, it was also of interest to investigate potential Na release in acid. 13.8 g of the wet cake was therefore dissolved in 6.67 ml HCl (37%). The mixture was left overnight with stirring for around 16 hours and thereafter filtered on a small Büchner with Munktell filter paper (class 00M). The obtained filter cake was thereafter washed with tap water at around 57 ℃. The resulting filtrate and wash water was sent for external macro elemental analysis with ICP-AES to investigate the release of Na from the filter cake in acidic conditions.

During the sixth and last cycle, an extensive wash of the cake was performed with a total target wash water ratio of 7.5. This condition is further referred to as extensive washing. The washing was conducted in batches and samples were collected separately for target wash water ratios of 1, 1.5, 2.5, 3.5, 5 and 7.5. An additional part of the filter cake was also dried at around 115 ℃ and saved for solid sample analyses with SEM-EDS and XRD.

3.2.2 Adsorption of sodium on aluminium silicates

An adsorption experiment was conducted on lab scale in order to investigate the adsorption potential of Na onto Al-silicates, which is one of the known filter cake components. In the experiment, a NaOH-solution with a similar concentration as in the Fe separation step was prepared by mixing NaOH (50%) with demineralised water. Three samples with different amounts of solid Al-silicates of similar type as the one known to be present in the filter cake were prepared in three beakers and mixed with a fixed volume of 50 ml NaOH-solution. The samples were left with stirring at room temperature for 23.5 hours. Experimental set-up data is summarised in Table 3.2.

Table 3.2: *Experimental set-up for adsorption experiment on Al-silicates.*

Sample	$V_{NaOH}[ml]$	$m_{solid}[g]$
Ads-1	50	1.25
Ads-2	50	2.51
Ads-3	50	5.02

The samples were thereafter filtered with vacuum on a Büchner funnel with Munktell filter paper (class 00M) and the resulting filtrates and filter cakes were collected. Volumes of filtrate and weights of wet filter cakes were noted. The filtrates were diluted with demineralised water and sent for external macro elemental analysis with ICP-AES in order to evaluate the amount of Na potentially adsorbed onto the solids. The three filter cakes were dried in an oven at around 115 ℃. The weight of wet and dried Al-silicate cakes was noted and used to calculate DS.

3.2.2.1 Washing of aluminium silicates

In order to also investigate the washing behaviour of Na from the Al-silicates, a washing experiment with three samples of equal amounts of solid Al-silicates was conducted. The samples with Al-silicates were prepared in beakers and mixed with a fixed volume of the same NaOH-solution as in the adsorption experiment. The samples were left with stirring in room temperature for 23.5 hours. The samples were thereafter filtered and washed with tap water using vacuum on a Büchner funnel with Munktell filter paper (class 00M). The washing was performed with tap water at a temperature of around 53 ℃. The washing was based on three different target wash water ratios, where the liquid content in the cake was estimated based on the mass of the trapped liquid in each cake. The set-up of the washing experiment is given in Table 3.3.

Table 3.3: *Experimental set-up for washing experiment of Al-silicates.*

Sample	$V_{NaOH}[ml]$	$m_{solid}[g]$	WW-ratio
Ads-4	50	2.50	1; 2.5; 5
Ads-5	50	2.51	1; 2.5; 5
Ads-6	50	2.52	1; 2.5; 5

As with the adsorption experiment, volumes of filtrate and wash water were measured as well as the weights of wet filter cakes. The filtrates and wash waters were diluted with demineralised water and sent for external macro elemental analysis with ICP-AES to evaluate the amount of Na that potentially was washed out from the cakes. Two filter cakes were dried in an oven at around 115 ℃. The third filter cake (3.64 g) was resuspended in 39 g week acid solution prepared by mixing HCl (1 M) and demineralised water. This was done to evaluate the effect of low pH on the Al-silicates and its release of Na. The slurry was left under stirring for one hour and thereafter filtered. The filtrate was collected, diluted and sent for external macro elemental analysis with ICP-AES.

3.3 Analyses of experimental results

This section describes the analytical procedure of liquid and solid samples that were internally analysed from the process reproduction as well as the adsorption on Al-silicates experiments.

3.3.1 Liquids analysis (Hach lange DR3900 + LCK cuvettes)

The tracking of Fe, Al and P concentrations in filtrate and wash water performed during the cycles was done using the Hach Lange DR3900 laboratory spectrophotometer together with LCK cuvettes. The cuvettes were prepared according to the methods described below and inserted to the spectrophotometer which is programmed to automatically determine the concentration. The wavelengths used was in the 320-1100 nm range [59].

3.3.1.1 Concentration determination using LCK cuvettes

Due to the sensitivity of the analysis, samples were first diluted with demineralised water to stay within the correct concentration range and the pH of the diluted samples was always checked. Samples outside the pH range was diluted using an appropriate amount of nitric acid (0.5 M) together with demineralised water.

In the Fe analysis, 2 ml of diluted sample was added to the LCK321-cuvette containing freeze-dried reagents. After the addition, the cuvette was closed and inverted until complete dissolution occurred. The cuvette was left for 15 minutes before it was inserted to the spectrophotometer. In the Al determination, 2 ml of an acidic acetate-buffered solution, 3 ml diluted sample and a small addition of an included powder was added to the LCK301 cuvette. The cuvette was inverted until complete dissolution occurred and was left for 25 minutes before it was inserted to the spectrophotometer. In the P analysis, 5 ml of the diluted sample was added to the LCK040-cuvette. The cuvette was inverted and left for 10 minutes before it was inserted to the spectrophotometer.

3.3.2 Solids analysis

Solid analysis with SEM-EDS and XRD were primarily performed on selected, dried filter cakes from the Fe separation step for the cycles without artificial alkaline solution. The studies were performed on solid inlet stream and outlet filter cake of cycle 5 with normal washing as well as outlet filter cake from cycle 6 with extensive washing. To enable comparison with the cycles with undesired Al-precipitates, analysis was also performed on the outlet filter cake of the last cycle (cycle 3) with artificial alkaline solution. The procedures and setup are described in more detail in following sections.

3.3.2.1 Analysis with SEM-EDS (Phenom ProX)

In order to perform cross-sectional analysis of solid samples with SEM-EDS, the dried samples of interest were embedded in epoxy. To be able to study single particles, some filter cake were milled to fine powders before the embedding. This was done for solid inlet stream and outlet filter cake of cycle 5 with normal washing as well as the outlet filter cake from cycle 6 with extensive washing from the cycles without artificial alkaline solution. It was also done on the final outlet filter cake from the cycles with artificial alkaline solution (cycle 3). Since the potential influence of washing on filter cake morphology was of great interest, non-milled pieces of filter cakes from cycle 5 with normal washing and cycle 6 with extensive washing (from cycles without artificial alkaline solution) were also embedded and studied. All the embedded samples were further grinded with sand papers of different roughness to polish the sample surface. At the beginning, water was used as cooling agent but it was later changed to ethanol to minimise cross-contamination of the samples (see Appendix A).

The SEM analyses were performed with a Phenom ProX instrument on one sample at a time. The samples were always cleaned with pressurised air before they were inserted to the instrument. In order to generate representative results, several areas of each sample were studied in SEM to understand morphology and types of particles present. Imaging were done with an accelerating voltage of 15 kV. Point analysis with EDS was performed on several location of each sample with repeated analyses on similar particles. This was mainly done in order to evaluate typical composition of common particles of each sample. Imaging and point analysis was done with a magnification of 2200x and 3800x. For the embedded samples with filter cake pieces, additional mapping of elements on a representative area were also performed with EDS. The mappings were done on a selected area with magnification of 2200x, map resolution of 256, pixel time of 50 and only one number of passes.

For all the completed analyses, unreasonable elements and elements with lower detection accuracy (<0.94) were excluded based on the known elemental compositions of the system. For the mapping results, C and O were also excluded, since they are known to be commonly present and thereby difficult to quantify correctly. They are also not considered as crucial elements in this investigation.

3.3.2.2 Analysis with XRD (D8 Advance)

To perform analysis of crystalline phases, the dried samples were milled into fine powders. The powders were thereafter pressed into a sample holder and placed in the sample chamber. The XRD analysis were performed in a D8 Advance instrument and the angle of incidence (2θ) was set to 5-80°. The samples studied with XRD were the inlet solids and outlet filter cake from cycle 5 with normal washing as well as the outlet filter cake from cycle 6 with extensive washing from cycles without artificial alkaline solution. XRD analysis was also done on the final outlet filter cake (cycle 3) from the cycles with recirculation of artificial alkaline solution.

After the XRD analysis, the generated spectra for each sample was plotted as an intensity vs. 2θ diffractogram and evaluated in the software *diffrac.suite eva*. A database of intensity diffractograms (COD) was available in the software. The elemental composition of the solids and filter cakes from EDS-analysis and externally performed ICP-MS was used to create a chemical filter for each sample, which were used together with the database to identify and distinguish possible crystalline phases. Firstly, the analysis was performed in automatic mode by the programme. Secondly, the results were evaluated and improved by manually matching the intensity peaks to diffractograms in the database. Finally, match lists of identified crystalline phases were summarised and used as matching filter to search for similar compounds in the different samples. The most feasible crystalline phases were kept as possible matches in the intensity diffractogram and further evaluated based on literature.

4
Results

The first part of the results chapter presents the main findings from analyses of the filter cake obtained from the cycles with artificial alkaline solution. However, these cycles will not be considered any further in the results. The following parts will instead provide a more detailed description of the general results obtained from the cycles without the use of artificial alkaline solution. When the results for the last set of cycles are presented, normal washing refers to the wash water ratio calculated as 2.33 which was used in cycle 5. The extensive washing refers to a total wash water ratio of 6.79 which was used in cycle 6.

4.1 Impact of aluminium accumulation due to the use of artificial alkaline solution

The cycles where artificial alkaline solution was used as an input to the Fe separation step were only performed in a total of three cycles. The cycles were stopped due to a discovered undesired Al accumulation in the filter cake when tracking the filtrate and wash water compositions. The filter cake from the last cycle was, however, analysed in SEM-EDS and XRD to study possible Al-precipitate and its possible influence on Na losses. This section will provide a brief presentation of the findings from these analyses with a special emphasis on comparing these results to the results from the cycles without artificial alkaline solution. It will also provide a more detailed explanation to the exclusion of artificial alkaline solution in the following cycles.

4.1.1 Impact of aluminium accumulation on sodium content

The accumulation of Al was not considered to be representative of the large scale process since a new component was believed to be introduced to the system. It was, however, of interest to investigate its influence on filter cake composition and Na losses. The compositions of Al and Na in the filter cakes from solid phase analysis with ICP-MS from cycle 3, with and without the use of artificial alkaline solution respectively, were therefore compared and the results, expressed as the ratio between cycle 3 with and cycle 3 without the solution, can be seen in Table 4.1.

Table 4.1: *Ratio of Al and Na from ICP-MS analysis of the filter cakes for cycle 3 with and without artificial alkaline solution respectively.*

Element	Ratio with/without
Al	3.9
Na	1.3

The ratio between contents presented in the table above shows that the resulting Al content was about four times larger in the filter cake when the artificial alkaline solution was used while the Na content was only slightly higher. Hence, the Al content was significantly larger in the cycle with artificial alkaline solution. The increase in Na content is not as large and cannot be explained by the Al accumulation.

4.1.2 Aluminium accumulation in filter cake components

The compositions of the two main filter cake components, Al-silicates and Fe-precipitates, were also studied in SEM-EDS to investigate the influence of Al accumulation on Na losses in specific particles. Cakes with similar washing conditions were only collected for cycle 3 with artificial alkaline solution and cycle 5 without artificial alkaline solution and cakes from different cycles are therefore compared. The results are shown in Table 4.2.

Table 4.2: *Mean atomic concentration in Al-silicates from cycle 3 (C3) with artificial solution and the content compared to cycle 5 (C5) without artificial solution. The compositions are normalised to the mean Si atomic concentration in the particles in each sample.*

Element	Mean C3 [%]	Ratio C3 with/C5 without
Si	100	1.00
Al	25	1.02
Na	10	0.58
K	7	1.06
Fe	4	0.27
Ca	2	0.20
P	1	0.09

It can be noticed that the Al content is only 2% higher which means that no clear Al accumulation have occurred near these particles. A larger increase in Al content was, however, noticed in the Fe-precipitates which can be seen in Table 4.3.

Table 4.3: *Mean atomic concentration in Fe-precipitates from cycle 3 (C3) with artificial solution and the content compared to cycle 5 (C5) without artificial solution. The compositions are the percentage of the mean Fe atomic concentration in the particles in each sample.*

Element	Mean C3 [%]	Ratio C3 with/C5 without
Fe	100	1.00
Na	42	0.80
Si	25	0.88
P	17	0.53
Al	15	1.71
Ca	14	0.41

As can be seen, the Al concentration is 70% higher in the cycles with artificial alkaline solution while the Na concentration is 20% lower for the same cycle. Thus, no effect of the Al accumulation on the Na losses was observed. It is, however, important to note that the differences in results also lies in the difference in number of cycles performed and the difference in washing conditions. These results can therefore only serve as an estimation of where the Al accumulation possibly occurred.

The results show that accumulation of Al did occur, but not on the Al-silicate surfaces. Instead, it was observed around Fe-precipitates. Furthermore, it did not have a significant effect on Na losses. In addition, no other Al-compounds in significant amounts or crystalline compounds containing Na was detected in XRD when compared to the cycles without artificial alkaline solution which suggests an amorphous nature of the formed Al-precipitate. Finally, the occurrence of precipitation can also be supported by the fact that the $NaAlO_2$ used for the preparation of the solution was proved to be unstable in tap water by the noticed precipitation during the first preparation of the solution, mentioned in section 3.2.1.1.

4.1.3 Exclusion of the artificial alkaline solution

Due to the Al accumulation, not expected in the large scale process, the results from the cycles with artificial alkaline solution could not be seen as representative for the process. Since the reason for the Al accumulation most likely was due to the use of chemicals which precipitates in the presence of tap water, it should not be expected to be a problem in the large scale process. Cycles mentioned below will therefore refer to the cycles without the use of artificial alkaline solution since the cycles mentioned above was not investigated further.

4.2 Operational results and steady state tracking

The operational results for the six cycles without artificial alkaline solution are summarised in this section. Values of measured DS, real wash water ratio used in each cycle as well as the normalised concentration of Na, Fe and P in filtrate and wash water can be found in Table 4.4. The normalised concentration of elements in the filtrate is expressed as a fraction of the concentration of the filtrate in cycle 6 meanwhile the concentration of elements in wash water is expressed based on the concentration in the filtrate for each cycle. The data is based on external macro elemental analysis with ICP-AES for all liquid streams in the system.

Table 4.4: *DS [%], real wash water ratio (WW-ratio) and concentration of Na, Fe and P in filtrate (F), expressed as a fraction of the concentration in cycle 6 (C6) [%], and in wash water (WW), expressed as a fraction of the concentration in the filtrate of each cycle [%].*

	C0	**C1**	**C2**	**C3**	**C4**	**C5**	**C6**
DS [%]	23.8	27.2	30.8	35.9	36.6	36.5	36.7
WW-ratio	1.42	2.45	2.51	2.46	2.35	2.33	6.79
$C_{Na,F}$[%]	46	86	89	79	93	99	100
$C_{Na,WW}$[%]	96	47	58	49	50	50	22
$C_{Fe,F}$[%]	100	100	100	100	100	100	100
$C_{Fe,WW}$[%]	100	100	100	100	100	100	100
$C_{P,F}$[%]	59	68	67	85	94	95	100
$C_{P,WW}$[%]	67	47	45	51	49	50	21

As can be seen in Table 4.4, the amounts of Na and P in the filtrate compared to cycle 6 are varying between the different cycles but a stabilisation can be noticed from cycle 4 to 6. This indicates that the system is close to reach steady state conditions. This is also supported by the stabilisation of DS for these three filter cakes. Further, it can be noticed that there are always Na and P present in the wash water for all cycles. On average, the detected concentration in the wash water is around half compared to filtrate concentration in cycle 1 to 5 but significantly lower in cycle 6 with extensive washing. Lastly, the concentration of Fe is found to be very stable in both filtrate and wash water for all cycles.

4.3 Sodium content at varying washing conditions

The effect of extensive washing on the Na losses was evaluated by looking at the concentration of Na in the filter cakes from cycles with different washing conditions. The cake composition were studied by external dissolution and analysis with ICP-MS and the result describes the mass of Na in the dissolved part of the filter cake per total dry cake mass. The effect of extensive washing is illustrated in Table 4.5 as the ratio of Na in the filter cake of cycle 6 with extensive washing compared to the filter cake of cycle 5 with normal washing.

Table 4.5: *Ratio of the concentration of Na in the filter cake of cycle 6 with extensive washing (WW-ratio of 6.79) compared to the concentration of Na in the filter cake of cycle 5 with normal washing (WW-ratio of 2.33).*

Cycle	ratio of Na in C5
C5	1
C6	0.62

From Table 4.5, it is seen that extensive washing in cycle 6 result in better removal of Na from the filter cake compared to normal washing in cycle 5. According to the ICP-MS analysis, it is possible to reduce the Na content in the filter cake with 38% by increasing the real wash water ratio to 6.79.

The effect of extensive washing was also evaluated by establishing a mass balance over the Fe separation step. In that way, it was also possible to evaluate the distribution of Na in the different streams. The mass balance were conducted for cycle 5 with normal washing and cycle 6 with extensive washing and the balance was based on all inlet and outlet streams. The liquid flows were analysed externally with ICP-AES and the solid phases were analysed by external dissolution and analysis with ICP-MS. The result are presented as the distribution of Na in all streams in the Fe separation step compared to the total inlet of Na for each cycle. The distribution of Na for cycle 5 with normal washing is presented in Figure 4.1. The deviation between total inlet and total outlet of cycle 5 was 2.6% of the total inlet of Na.

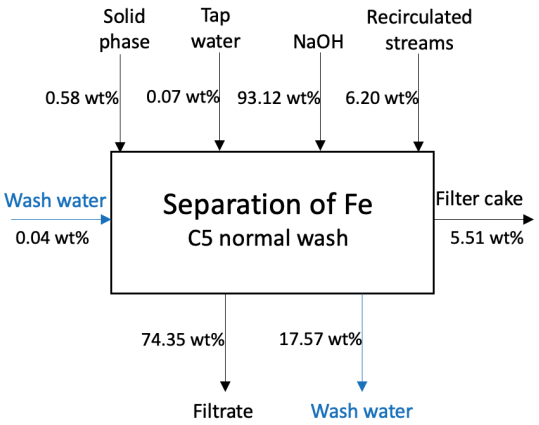

Figure 4.1: *Amounts of Na in inlet and outlet streams in the Fe separation step expressed as wt% of total inlet for cycle 5 (C5) with normal washing (WW-ratio of 2.33).*

As can be seen in Figure 4.1, 5.51 wt% of the Na added to cycle 5 is undesirably trapped in the filter cake while 17.57 wt% is removed by washing. To be able to evaluate the effect of extensive washing, a similar figure with the distribution of Na was also established for cycle 6 with extensive washing and the result is shown in Figure 4.2. By comparing the total inlet and outlet, the deviation of cycle 6 was 2.7% of the total inlet of Na.

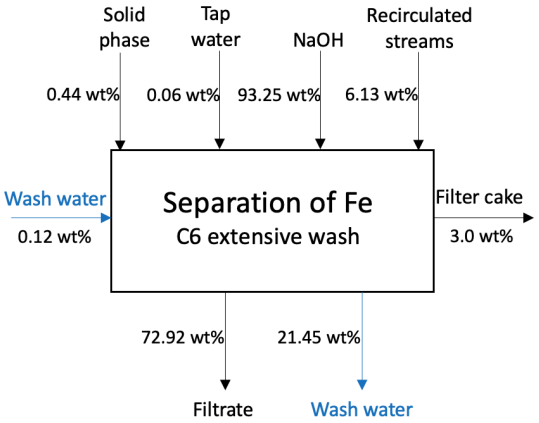

Figure 4.2: *Amounts of Na in inlet and outlet streams in the Fe separation step expressed as wt% of total inlet for cycle 6 (C6) with extensive washing (WW-ratio of 6.79).*

As seen in Figure 4.2, the amounts of Na trapped in the filter cake is 3 wt% of the total inlet of Na to cycle 6. By comparing the result with Figure 4.1, it can be noticed that more Na is washed out from the filter cake in cycle 6 with extensive washing than in cycle 5 with normal washing. This implies that it is possible to reduce the losses by increasing the washing of the filter cake.

By further comparing the inlet distribution of Na between the different inlet streams in Figure 4.1 and Figure 4.2, it can also be seen that they are similar in the two cycles. It can also be noticed that the largest flow of Na is related to the addition on NaOH as intended. Additionally, it should also be mentioned that the total concentration of Na in the reactor were kept similar in the two cycles.

By comparing the results from the ICP-MS analysis with the results from the mass balance, it is seen that both approaches shows a decreased amount of Na trapped in the filter cake between cycle 5 with normal washing and cycle 6 with extensive washing. Thus, this indicates that extensive washing decreases the Na losses to the filter cake.

4.4 Acidic exposure of the filter cake

As described in section 3.2.1.4.2, it was of interest to evaluate the effect of acidic conditions on the release of Na from the filter cake. The release of Na in acidic conditions from the filter cake in cycle 5 was investigated by dissolving a minor part in HCl (37%) during 16 hours. The results from external macro elemental liquid analysis with ICP-AES were used to calculate the amount of Na released in acidic conditions compared to the total concentration of Na in the inlet to cycle 5, expressed in wt%. The results are illustrated in Figure 4.3.

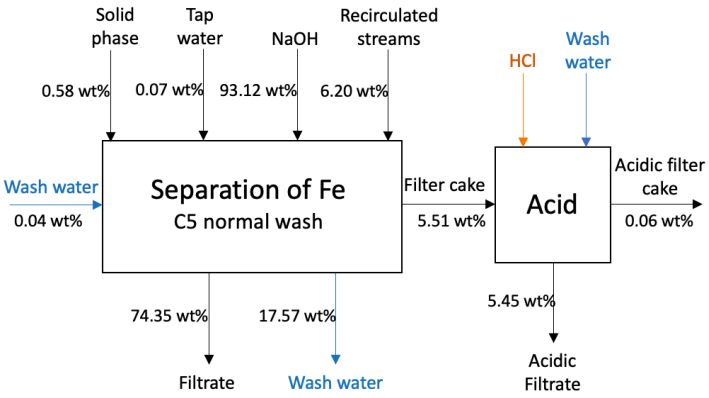

Figure 4.3: *Amounts of Na in inlet and outlet streams in the Fe separation step cycle 5 and the release of Na from the filter cake after 16 hours in acidic conditions with HCl (37%). All values are expressed as wt % of total inlet to cycle 5.*

As can be seen in Figure 4.3, it was possible to almost fully release the Na trapped in the filter cake by dissolving it in acid. At the same time, sufficient amounts of acidic filter cake were left after the acidic exposure. Since almost all of the Na in the filter cake were released in the acidic exposure, the majority of the trapped Na is associated with the part of the cake which is possible to dissolve in acid.

4.5 Washing of the filter cake

To evaluate the washing procedure, samples of filtrate and wash water from cycle 6 were collected and analysed with ICP-AES for target wash water ratios of 0, 1, 1.5, 2.5, 3.5, 5 and 7.5. The wash water ratios were thereafter recalculated based on the real DS of the filter cake according to the method described in section 3.2.1 and C* was calculated according to equation 2.3. The obtained washing curve is shown in Figure 4.4.

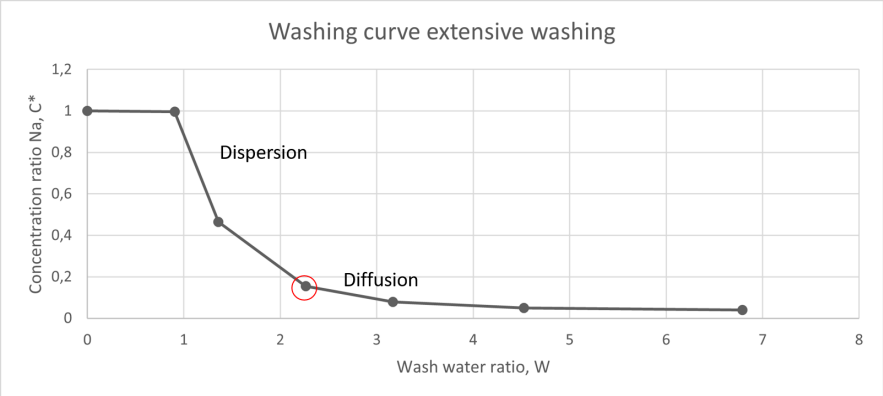

Figure 4.4: *Washing curve based on the filtrate and wash water concentrations from cycle 6 during the extensive washing with corrected wash water ratios. The shift from dispersion region to diffusion region is also marked.*

It is seen that almost pure mother liquor was obtained during the first wash. Thereafter, a clear dispersion behaviour can be observed from a wash water ratio of 0.91 to a wash water ratio of 2.26. The obtained results shows that Na can be targeted by additional washing compared to normal washing conditions. However, at wash water ratios larger than 2.26, the washing becomes less effective.

4.6 Investigation of aluminium silicates

One of the known filter cake components, Al-silicates, was investigated with respect to adsorption potential and washing behaviour. The results are presented below.

4.6.1 Sodium losses to aluminium silicates

In order to investigate the possibility of adsorption of Na onto Al-silicates, experiments were performed as described in section 3.2.2 and the result is presented in this section. For the adsorption experiment with three different amounts of Al-silicates, DS, initial and final volumes of NaOH-solution and initial and final dry masses of Al-silicates are summarised in Table 4.6.

Table 4.6: *Initial and final volumes of NaOH-solution (L) as well as initial and final dry masses of Al-silicates (S) in the adsorption experiment. The table also includes DS [%] and changes in volumes [%] and dry masses [wt%] during the experiment.*

Sample	DS[%]	$V_{L,in}[ml]$	$V_{L,out}[ml]$	ΔV_L[%]	$m_{S,in}[g]$	$m_{S,out}[g]$	$\Delta m_S[wt\%]$
Ads-1	62	50	48.0	-4.0	1.25	1.11	-11.2
Ads-2	62	50	45.5	-9.0	2.51	2.34	-6.8
Ads-3	62	50	45.0	-10.0	5.02	4.73	-5.8

In Table 4.6, it is found that both volumes of solution and dry masses of solids are decreasing for all samples during the experiment. The changes in volumes shows that liquid is trapped in the solids. This can partly be explained by that the Al-silicates naturally will take up some liquid as the dry solids are mixed with the solution, which will reduce the liquid volume in the beaker and affect the DS of the Al-silicates. As showed in Table 4.6, the DS has decreased from near 100% before the experiment to 62% afterwards. At the same time, the change in masses indicates that the solids are partly dissolved during the experiment.

In the washing experiment, described in section 3.2.2.1, three adsorption attempts with equal amounts of Al-silicates were first performed. The initial and final volumes of NaOH solution for the samples are summarised in Table 4.7.

Table 4.7: *Initial and final volumes of NaOH-solution in repeated adsorption experiment with an Al-silicate mass of 2.5 g. The table also includes the change in volume [%] during the experiment.*

Sample	$V_{NaOH,in}[ml]$	$V_{NaOH,out}[ml]$	$\Delta V_{NaOH}[\%]$
Ads-4	50	46.5	-7.0
Ads-5	50	47.0	-6.0
Ads-6	50	47.0	-6.0

As can be seen in Table 4.7, the volumes of NaOH-solution are decreasing in all three samples. Yet, it is noticed that the change in Ads-4 is slightly larger than in Ads-5 and Ads-6. By further comparing these samples with Ads-2 (same operating conditions) in Table 4.6, it is seen that the change in volume are even larger in Ads-2. However, even if there is a deviation of liquid left in the solids between the samples, it is still clear that a part of the liquid was trapped in the Al-silicates during the adsorption experiments.

To illustrate adsorption of Na for different adsorbent dosage of Al-silicates, an adsorption curve was created based on the result from the adsorption experiment. The result is shown in Figure 4.5 together with a curve illustrating the total Na losses in the system, which also account the losses associated with the liquid trapped in the Al-silicate filter cake.

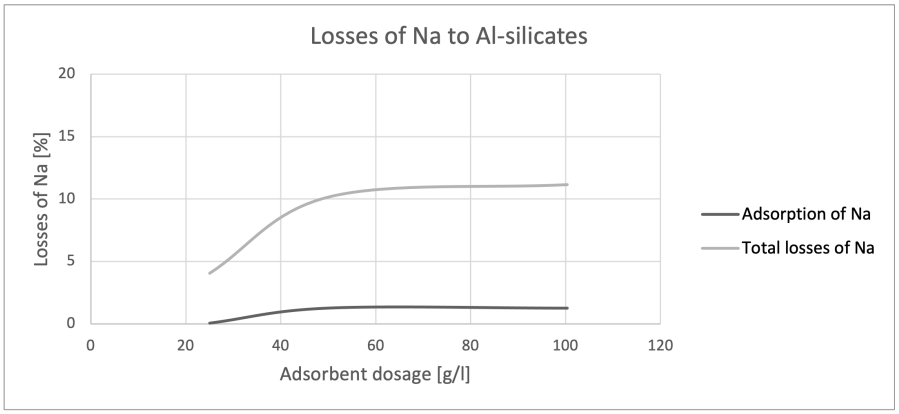

Figure 4.5: *Adsorption of Na on Al-silicates as well as total losses of Na to Al-silicates based on experimental data.*

In Figure 4.5, it is well illustrated that the adsorption of Na is sufficiently low in general, with only a maximum adsorption of Na of 1.3% at a adsorbent dosage of 100 g/l. It can also be seen that the adsorption is most likely not dependent on adsorbent dosage, since the curve is flat. At the same time, it can be noticed that the maximum total loss of Na to the Al-silicates is as high as 11%. By comparing the two curves in the figure, it is clear that the majority of the Na losses to the Al-silicates are associated with the liquid trapped in the Al-silicate filter cake and not adsorption. Therefore, it is likely that adsorption represents a negligible phenomena in the investigated system.

It is possible to evaluate the adsorption behaviour and potentially also adsorption mechanisms of a system by combining experimental data with isotherms models, such as Langmuir and Freundlich. However, due to the negligible adsorption behaviour, it was decided to not continue the study of adsorption.

4.6.2 Washing of aluminium silicates

The washing of Al-silicates was evaluated based on the results from the washing and acidic exposure experiments on Al-silicates, described in section 3.2.2.1. The amount of trapped NaOH-solution during the repeated adsorption experiment with Al-silicates were estimated to be slightly higher for Ads-4 than for Ads-5 and Ads-6. The amount of wash water, which was based on the amount of liquid trapped by the solid during the adsorption part of the experiment, added for the washing was therefore larger in Ads-4 (Table 4.7). This can be seen in Table 4.8 where inlet and outlet wash water amounts are presented.

Table 4.8: *Inlet and outlet weight of the wash water used in the wash of Al-silicates. The experiment number followed by the wash water ratio are marked in the table.*

Sample - ww ratio	**Wash water in [g]**	**Wash water out [g]**
Ads-4-ww-1	3.7	4
Ads-5-ww-1	3.1	3.2
Ads-6-ww-1	3.31	3.53
Ads-4-ww-2.5	5.5	5.5
Ads-5-ww-2.5	4.7	4.6
Ads-6-ww-2.5	4.69	4.65
Ads-4-ww-5	9.2	9.1
Ads-5-ww-5	7.8	7.9
Ads-6-ww-5	7.82	7.58

It can also be noticed that the deviation between the experiments was small in the first wash but increased for higher wash water ratios. The washing of these samples were also tracked by analysing the outlet concentration of filtrate and wash water and a washing curve was established, presented in Figure 4.6.

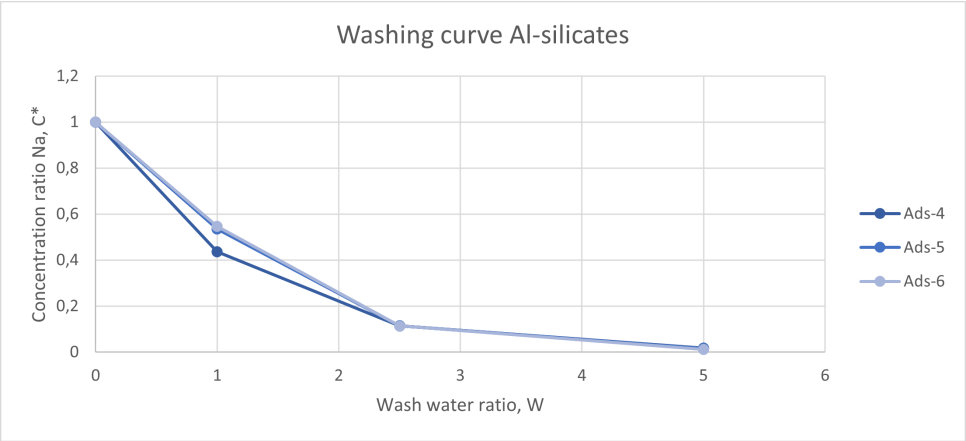

Figure 4.6: *Washing curve for the Al-silicates from sample Ads-6 obtained in one of the adsorption experiments.*

The same behaviour was observed for Ads-5 and Ads-6, while Ads-4 deviated slightly from the other two experiments. However, this is an effect of the difference in addition of wash water that was presented in Table 4.8. The diffusion region can be observed to start somewhere between a wash water ratio of 1 and 2.5 but the correct value cannot be determined since important data points in this region are missing. It is also seen that almost all accessible Na have been washed out at a wash water ratio of 5. Comparing the washing behaviour of the Al-silicates with the washing behaviour of the filter cake (Figure 4.4), the dispersion region of the Al-silicates appears to occur already during the first wash in contrast to the filter cake in which almost pure mother liquor is obtained during the first wash.

The effect of washing on the Al-silicates was further evaluated based on comparing the obtained Na from the washing to the total inlet of Na. As mentioned, sample Ads-6 was also resuspended in acidic conditions to evaluate any possible release of Na. The exposure showed that a significant part of the cake was still kept undissolved. In addition, only a minor part of the Na was released in the acidic conditions. The results for the washing and the acidic exposure are presented in Table 4.9.

Table 4.9: *Na trapped by the Al-silicates after the adsorption experiment, after the washing and after the acidic exposure experiments based on the total inlet of Na in the NaOH-solution and wash water.*

Sample	**Inlet** [%]	**After filtration** [%]	**After wash** [%]	**After acid** [%]
Ads-4	100	5.31	0.04	-
Ads-5	100	5.77	0.50	-
Ads-6	100	9.49	4.06	3.97

It is clearly seen in the table that the small scale of the experiments as well as the uncertainties in the analysis method results in large deviations in the experimental results. However, most of the Na contained in the liquid trapped by the Al-silicates seems to be removed during the washing.

4.7 Solid sample analyses

The SEM-EDS and XRD analyses of the filter cakes from cycle 5 and cycle 6 as well as the solid inlet stream of cycle 5 are the focus of this section. It is divided into four main parts. First, the morphology observed in SEM is described. Thereafter, the compositions as well as the distribution of the main elements in the particles are presented. At last, the crystalline structures detected in XRD are presented.

4.7.1 Morphology of solid samples

The morphology of the filter cakes after normal washing, after extensive washing as well as the solid inlet stream to the Fe separation step were studied in SEM and the results are presented below.

4.7.1.1 Morphology of the solid inlet stream

The solid inlet stream was analysed in SEM in order to compare the structural differences before and after the NaOH addition in the Fe separation step. Only one particle type containing Na was found. These particles were dominated by Si and were therefore believed to be the Al-silicates that were expected to be found. An overview of the crushed solid inlet stream sample is shown in Figure 4.7.

(a) 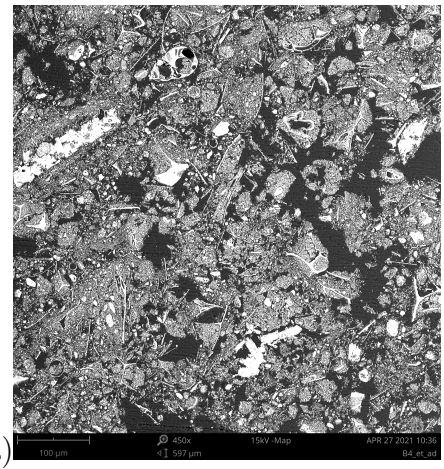

(b) 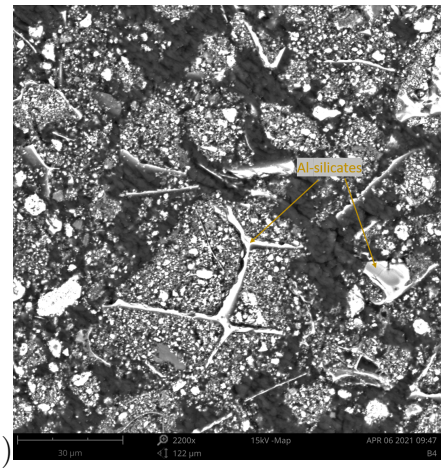

Figure 4.7: *Overview of particles in the crushed sample of the solid inlet stream to the Fe separation step with (a) magnification 450x (b) magnification 2200x and with Na containing Al-silicates marked.*

As can be seen. Al-silicates were observed in two different shapes. However, both types had similar compositions. It should also be noted that this sample is crushed and the porosity and structure of the sample cannot be directly compared to the morphology of the samples described in section 4.7.1.2 and 4.7.1.3. Other particles were also present in the sample but did not contain significant amounts of Na.

4.7.1.2 Morphology of the filter cake after normal washing

Particles of different sizes and forms were observed in the sample after normal washing conditions. Some particles were smaller and more compact while others appeared like longer strings, similar to the ones found in the solid inlet stream. Both porous and less porous parts of the filter cake after normal washing were observed as can be seen in the overviews in Figure 4.8.

(a) 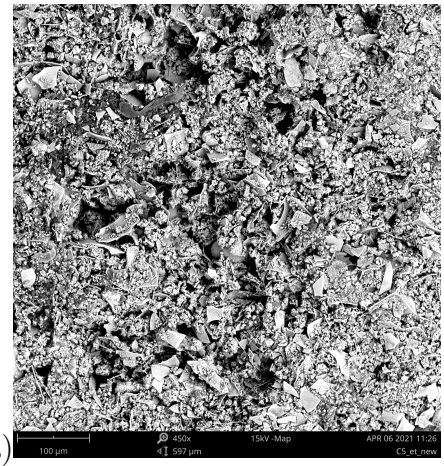

(b) 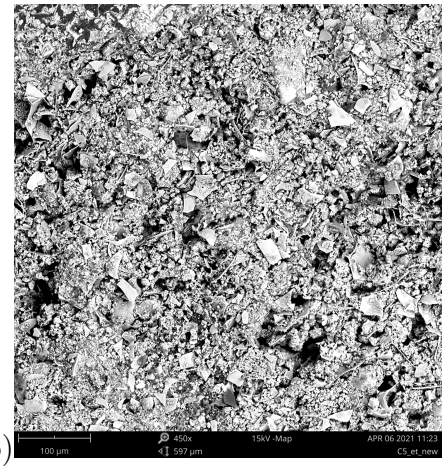

Figure 4.8: *Overviews of the filter cake at different areas after normal washing, both (a) and (b) at a magnification of 450x.*

Three main Na containing particles were found in the filter cake after normal washing conditions. These particles were either dominated by Fe (Fe-precipitate), Si (Al-silicates) or Ca (Ca-precipitate). SEM-micrographs of the main particles marked are shown in Figure 4.9.

(a) 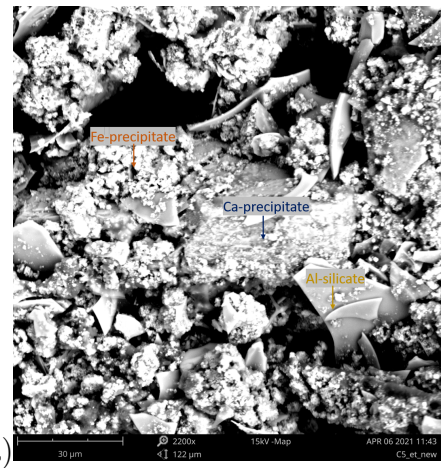

(b) 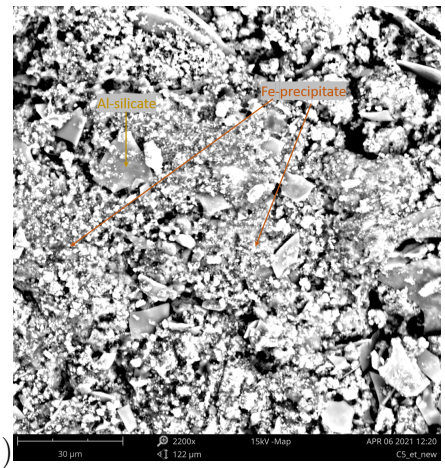

Figure 4.9: *Micrographs of the cake after normal washing grinded with ethanol at a magnification of 2200x. (a) Fe-precipitate, Ca-precipitate and Al-silicates (b) Fe-precipitate and Al-silicates*

As expected, most of the particles were Fe-precipitates followed by Al-silicates. A minor part of the particles were those dominated by Ca. It can also be noted that the different shapes of the Al-silicates are present in this sample as well as in the solid inlet stream (section 4.7.1.1).

4.7.1.3 Morphology of the filter cake after extensive washing

The morphology of the filter cake after extensive washing had no clear differences compared to the filter cake after normal washing. Two overview SEM-michrographs can be seen in Figure 4.10.

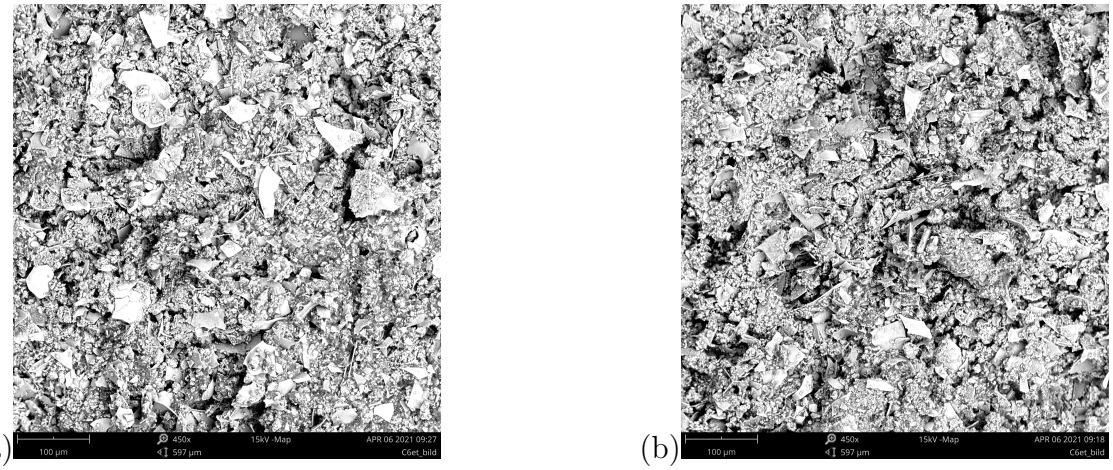

Figure 4.10: *Overviews of the filter cake at different areas after extensive washing, both (a) and (b) at a magnification of 450x.*

The three types of Na containing particles found after normal washing were also found in the filter cake after extensive washing. Examples are shown in more detail in Figure 4.11.

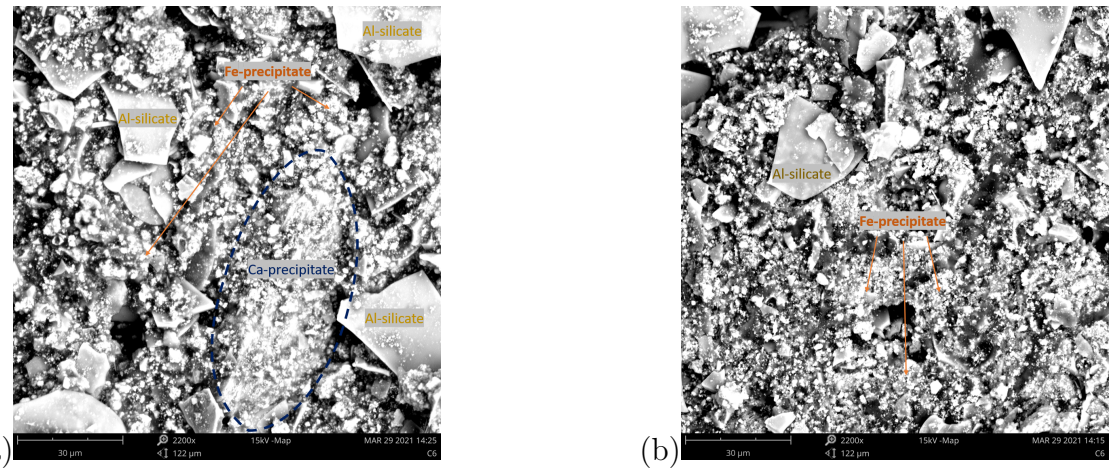

Figure 4.11: *Micrographs of the cake from extensive washing grinded with ethanol at a magnification of 2200x. (a) Fe-precipitate, Ca-precipitate and Al-silicates (b) Fe-precipitate and Al-silicates.*

Comparing Figure 4.9 and Figure 4.11, it can be seen that the particles have the same shape, size and form. No significant difference with respect to distribution of particle types was neither noted when the filter cakes with different washing conditions were compared, which means that the Fe-precipitates occupied, as expected, the largest part of the cake.

4.7.2 Composition of solid samples

This section provides the results obtained from analyses with SEM-EDS of the two filter cakes at different washing conditions as well as the solid inlet stream in cycle 5. All compositions presented in this section are reported on a C and O free basis and are based on point analyses of several particles in each sample. The distribution of elements in certain areas of the filter cakes are presented as EDS-mappings. These mappings were performed in one specific area for each filter cake. This means that each mapping of an individual element in one specific filter cake can be compared to all other mappings from the same sample. These areas can be seen in Appendix B.

4.7.2.1 Composition of the solid inlet stream

Al-silicates, known to be present in the filter cake, were also observed in the filter cake from the solid inlet in cycle 5. These particles were analysed with EDS to compare the composition of solids before and after the NaOH addition. The mean atomic concentration of the main elements in the Al-silicates entering the reactor are presented in Table 4.10.

Table 4.10: *Minimum, maximum and mean atomic concentration of main elements in Al-silicates from the inlet of the separation of Fe based on 10 point measurements normalised with the mean atomic concentration of Si. The standard deviation, σ, and the variance, σ^2, for the data points are also displayed.*

Element	**Min** [%]	**Max** [%]	**Mean**	σ	σ^2
Si	92	105	100	0.031	0.00099
Al	26	27	26	0.0018	3.2e-6
Na	6	14	10	0.016	0.00027
P	5	13	8	0.016	0.00027
K	5	9	7	0.016	0.00027
Fe	4	7	5	0.0071	5.1e-5
Ca	5	13	3	0.0034	1.2e-5

The results in Table 4.10 shows that Na is the third most dominating component in the Al-silicates prior to the separation of Fe based on average normalised composition. These results will further on be compared to the composition of the Al-silicates after the separation of Fe.

4.7.2.2 Composition of the filter cake after normal washing

The three main particles present in the sample, dominated by Fe, Si or Ca respectively, were analysed with EDS in several representative points, as described in section 3.3.2.1, and the average atomic concentration was thereafter calculated. The average composition of the Al-silicates, expressed as the percentage of the average atomic concentration of Si, are presented in Table 4.11.

Table 4.11: *Minimum, maximum and mean atomic concentration of main elements in Al-silicates after normal washing based on 25 point measurements normalised with the mean atomic concentration of Si. The standard deviation, σ, and the variance, σ^2, for the data points are also presented in the table.*

Element	**Min [%]**	**Max [%]**	**Mean [%]**	σ	σ^2
Si	64	120	100	0.084	0.0071
Al	15	30	24	0.021	0.00045
Na	8	33	17	0.033	0.0011
Fe	5	36	15	0.048	0.0023
Ca	2	20	9	0.028	0.00077
P	0	17	6	0.024	0.00059
K	3	10	6	0.0097	9.4e-05

As can be seen in the table, Na is the third most dominating element in the Al-silicates after normal washing based on average normalised composition. It is important to note that the Al-silicates are already present at the inlet of the Fe separation and the ratio between the Na and Si after normal washing has increased compared to the ratio of the inlet stream presented in Table 4.10. This indicates that some additional Na is trapped in the Al-silicates during the separation of Fe. In addition, the contents of Fe and Ca in the Al-silicates have also increased compared to the inlet solid stream analysis. The distribution of Na and Si after normal washing can be compared in Figure 4.12.

(a) 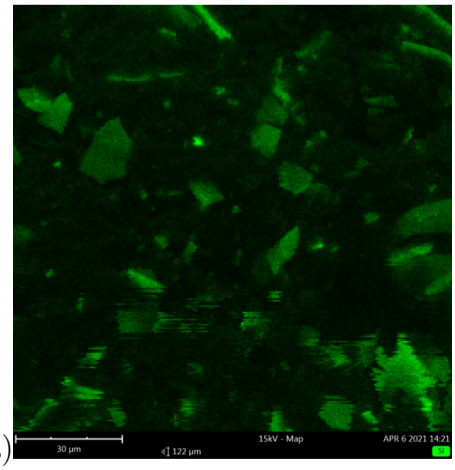

(b) 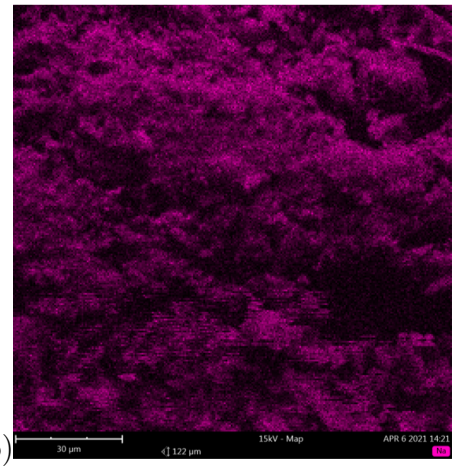

Figure 4.12: *Distribution of (a) Si and (b) Na, in same area of the filter cake after normal washing. No clear similarities can be observed.*

It can be seen that Na is more evenly distributed throughout the area of the mapping while the Si are more concentrated in specific particles corresponding to the shape of the Al-silicates shown in Figure 4.9. No clear similarities between the Na and Si distribution can, however, be distinguished. Further, the EDS analysis was also done on Fe-precipitates. The average composition based on the mean atomic concentration of Fe are presented Table 4.12.

Table 4.12: *Minimum, maximum and mean atomic concentration of main elements in Fe-precipitates after normal washing based on 25 point measurements normalised with the mean atomic concentration of Fe. The standard deviation, σ, and the variance, σ^2, for the data points are also shown.*

Element	**Min** [%]	**Max** [%]	**Mean** [%]	σ	σ^2
Fe	68	154	100	0.081	0.0065
Na	25	82	52	0.057	0.0032
Ca	14	69	35	0.52	0.0027
P	17	51	33	0.034	0.0011
Si	19	48	28	0.028	0.00076
Al	0	13	9	0.012	0.00014

It can be seen that the Na is the second most dominating element in the Fe-precipitates after normal washing based on average normalised composition. Furthermore, the distribution of Na and Fe in the same part of the filter cake can be compared in Figure 4.13.

(a) (b)

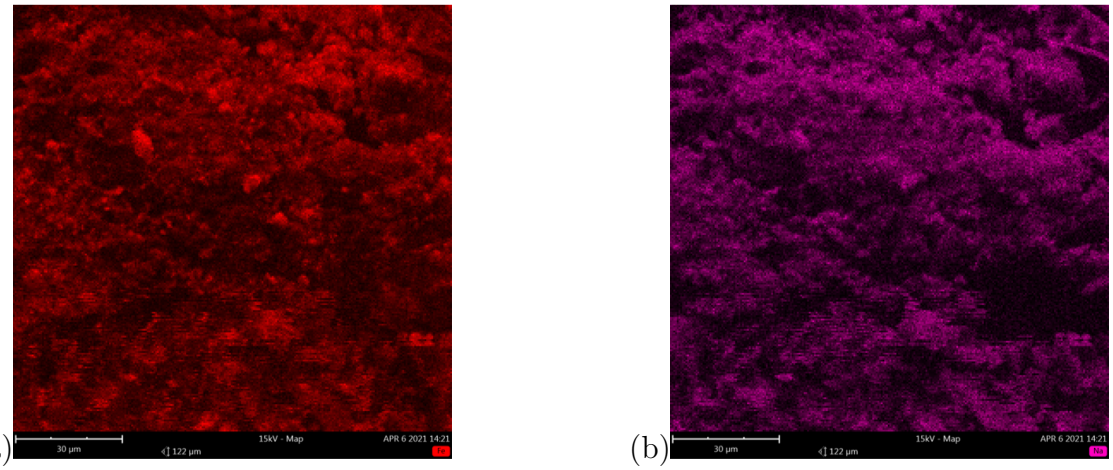

Figure 4.13: *Distribution of (a) Fe (b) Na, in same area of the filter cake after normal washing.*

It can be seen that both elements in Figure 4.13 appears as evenly distributed throughout the area of the mapping. Further, Na was found in significant amounts in the Ca-precipitates as can be seen in Table 4.13, where the average composition based on the mean Ca atomic concentration, is presented.

Table 4.13: *Minimum, maximum and mean atomic concentration of main elements in Ca-precipitates after normal washing based on eight point measurements normalised with the mean atomic concentration of Ca. The standard deviation, σ, and the variance, σ^2, for the data points are also presented.*

Element	**Min [%]**	**Max [%]**	**Mean [%]**	σ	σ^2
Ca	70	140	100	0.073	0.0054
P	56	91	74	0.032	0.0010
Na	29	102	67	0.084	0.0071
Fe	25	54	43	0.028	0.00080
Si	17	34	26	0.018	0.00032
Al	0	8	2	0.011	0.00013

The obtained results, based on average normalised values, shows that Na is the third most dominating element in the Ca-precipitates after normal washing. In addition, the distribution of Ca and Na can be compared in Figure 4.14.

(a) 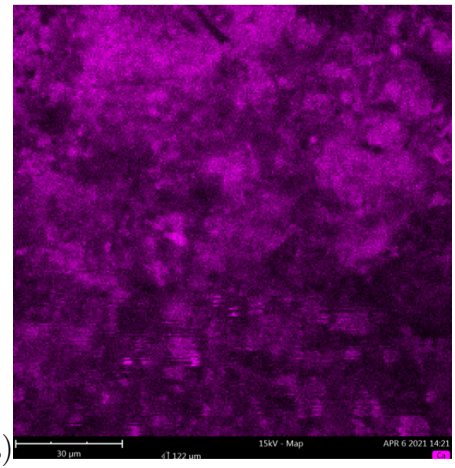

(b) 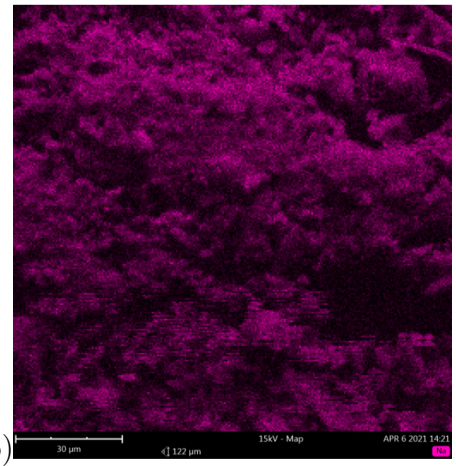

Figure 4.14: *Distribution of (a) Ca and (b) Na, in same area of the filter cake after normal washing. No clear similarities can be observed.*

As can be seen, Ca is also distributed over the entire area of the mapping after normal washing as was also noticed for Na and Fe. Hence, no clear similarities in distribution were observed for any of the elements investigated in this section.

4.7.2.3 Composition of the filter cake after extensive washing

The compositions in the three Na containing particles after the extensive washing were checked with EDS and compared to the composition in the corresponding particles after normal washing. The result for the Al-silicates is presented in Table 4.14.

Table 4.14: *Minimum, maximum and mean atomic concentration of main elements in Al-silicates after extensive washing based on 25 point measurements normalised with the mean atomic concentration of Si. The standard deviation, σ, and the variance, σ^2, for the data point are also shown.*

Element	**Min [%]**	**Max [%]**	**Mean [%]**	σ	σ^2
Si	55	115	100	0.081	0.0065
Al	12	27	22	0.026	0.00067
Fe	6	57	15	0.066	0.0044
Na	0	24	11	0.045	0.0020
K	4	15	8	0.016	0.00025
P	0	45	4	0.054	0.0029
Ca	0	15	4	0.021	0.00046

It can be seen that Na is the fourth most dominating element in the Al-silicates after the extensive washing, compared to being the third most dominating in the Al-silicates after the normal washing. The distribution of Si and Na after extensive washing are shown in 4.17.

(a) 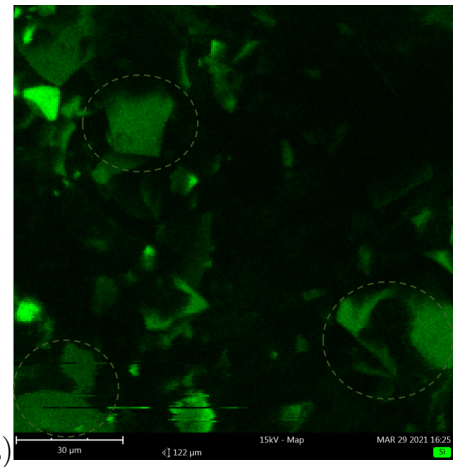

(b) 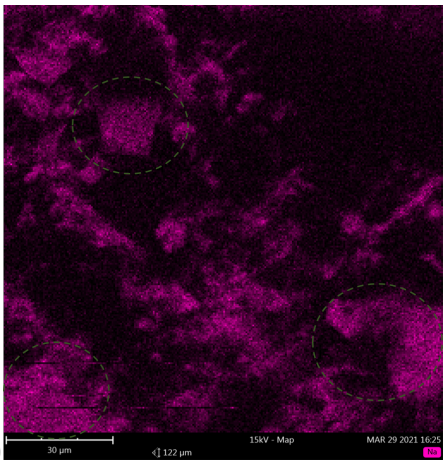

Figure 4.15: *Distribution of (a) Si and (b) Na, in the same are of the filter cake after extensive washing. Some areas to compare are marked in the figure.*

It can be seen that the Na is more distinct in some areas of the mapping compared to the normal washing conditions (Figure 4.15) where it was distributed evenly over the entire area. Some of the areas of Na after extensive washing are also the same as the ones for Si. Some of these areas are also marked in the figure. The Si distribution in the mapping was mainly related to the Al distribution (Appendix C). Further, Na was also found in the Fe-precipitates after the long wash. The average Fe-precipitate composition after extensive washing is presented in Table 4.15.

Table 4.15: *Minimum, maximum and mean atomic concentration of main elements in Fe-precipitate after extensive washing based on 23 point measurements normalised with the mean atomic concentration of Fe. The standard deviation, σ, and the variance, σ^2, for the data point are also presented.*

Element	Min [%]	Max [%]	Mean [%]	σ	σ^2
Fe	68	122	100	0.055	0.0030
Si	26	73	39	0.043	0.0019
Na	0	64	38	0.048	0.0023
Ca	18	51	35	0.030	0.00088
P	20	41	32	0.021	0.00046
Al	0	19	9	0.018	0.00034

As can be seen, Na is the third most dominating element in the Fe-precipitates after the extensive wash based on average normalised composition. This can be compared to the results from normal washing in which the Na was the second most dominating element (Table 4.12). It can also be noticed that the composition of other elements in the particles remain rather constant but the Si average, expressed as the percentage of Fe concentration, has increased after the extensive washing. The distribution of Na and Fe in the sample were also compared, shown in Figure 4.16.

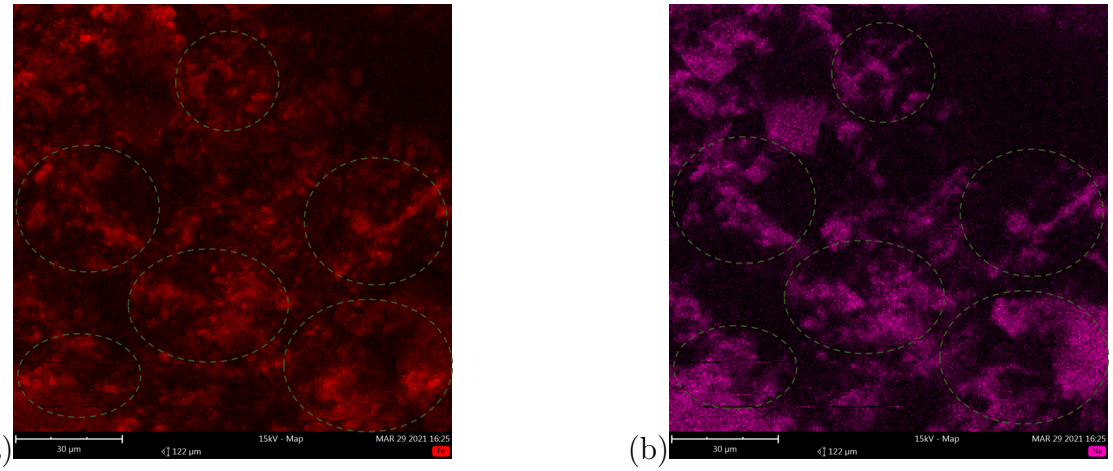

Figure 4.16: *Distribution of (a) Fe and (b) Na, in the same area of the filter cake after extensive washing. Some overlapping areas are marked.*

Similarities in Fe and Na distribution after extensive washing can be noticed in some areas of the mapping that are marked in the figure. This results deviates from the results seen after normal washing (Figure 4.13) in which both elements were evenly distributed with no clear similarities. The Fe can especially be noticed to be less distributed after the longer wash than after the normal wash. Furthermore, Na was also found in the Ca-precipitates after the extensive washing as can be seen in Table 4.16 where the average composition is presented.

Table 4.16: *Minimum, maximum and mean atomic concentration of main elements in Ca-dominated particles after extensive washing based on nine point measurements normalised with the mean atomic concentration of Ca. The standard deviation, σ, and the variance, σ^2, for the data point are also displayed.*

Element	**Min [%]**	**Max [%]**	**Mean [%]**	σ	σ^2
Ca	65	128	100	0.088	0.0077
P	55	74	67	0.030	0.00091
Si	11	28	19	0.027	0.00071
Fe	0	32	17	0.041	0.0017
Na	0	49	16	0.067	0.0045
Al	0	7	2	0.012	0.00014

As can be seen in the table, the Na is the fifth most dominating element in the Ca-precipitates after the extensive wash compared to being the third most dominating after the normal wash (Table 4.13). It can also be noticed that the Fe concentration has decreased significantly during the wash. Lastly, the distribution of Ca and Na in the same area after the extensive wash should be compared, presented in Figure 4.17.

(a) 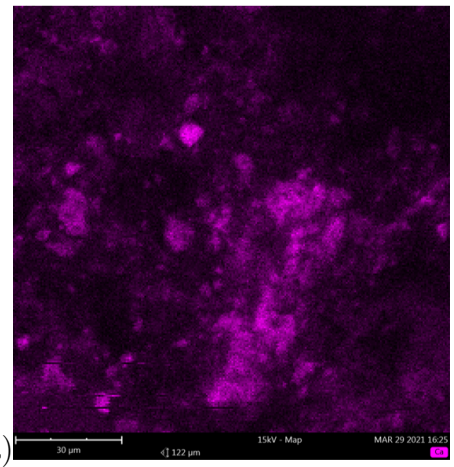

(b) 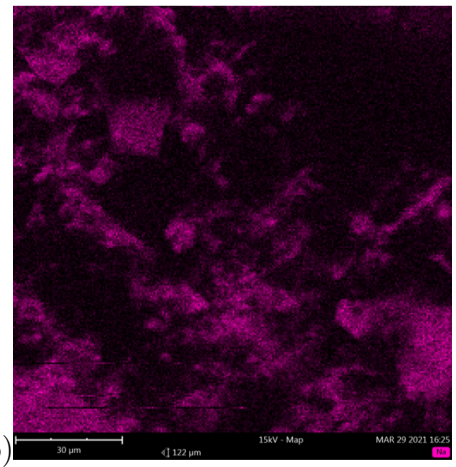

Figure 4.17: *Distribution of (a) Ca and (b) Na, in the same area of the filter cake after extensive washing. The elements are not associated.*

The obtained EDS-mapping results shows that Na and Ca are not cleary associated after extensive washing. An association of Ca near P was, however, more clearly seen (Appendix C). By further comparing all mapping results after extensive washing, it can be noticed that the distribution of Na is more comparable to the distribution of Fe and Si than to the distribution of Ca.

4.7.2.4 Washing behaviour of different particle types

To get an overview of the Na content in different particle types after varying washing conditions, the results from normal (cycle 5) and extensive (cycle 6) washing were summarised. Since some Na was already present in solid form in the Al-silicates

entering the reactor, this content was not expected to be washed out from the particles. The difference between normal and extensive washing in these particles was therefore also based on the concentration increase from the solid inlet. The washing results for the three particles found in the solid samples are presented in Table 4.17.

Table 4.17: *Comparison of the mean Na content in Si, Fe and Ca particles obtained from EDS-analysis after normal and extensive washing. For the Al-silicates, the original concentration from the solid inlet stream was not considered as available for washing and was therefore also subtracted for comparison, expressed in brackets.*

Sample	**Na/Si**	**Na/Fe**	**Na/Ca**
Solid inlet	10	-	-
Normal wash (C5)	17 (7)	52	67
Extensive wash (C6)	11 (1)	38	16
"Washed out" [%]	35 (86)	27	76

From the obtained results, the largest Na ratio for normal washing conditions is observed in the Ca-precipitates while the largest Na ratio for extensive washing conditions is found in the Fe-precipitates. The smallest ratio can be observed in the Al-silicates after both washes.

It can also be noticed that if only the total concentrations of the cakes from normal and extensive washing are being compared, a minority of the Na present in cycle 5 has been washed out in cycle 6. However, since at least some of the Na in the solid inlet stream particles is considered to be inaccessible for the washing, most of the accessible Na have been washed out from the Al-silicates. Further, Ca-precipitates appears to be rather easy to wash while Fe-precipitates still contains a significant amount of Na after extensive washing.

4.7.3 Crystalline structures of solid samples

In order to identify crystalline structures in the Fe separation step, studies with XRD were performed on the solid inlet stream and outlet of cycle 5 with normal washing and the outlet from cycle 6 with extensive washing. The identification of crystalline structures was based on the elemental results from external elemental analysis of the filter cakes with ICP-MS. Due to the complexity of the spectrum, the number of identified structures were limited. The structures found in XRD that were well detected were categorised based on the identified particle types in section 4.7.1 and the number of each precipitate are summarised in Table 4.18.

Table 4.18: *Types of crystalline structures possibly found in XRD in solid inlet and filter cake outlet in cycle 5 with normal washing as well as filter cake outlet in cycle 6 with extensive washing.*

Sample	Al-silicates	Ca-precipitate	Na-precipitate
Solid inlet	3	1	-
Normal wash (C5)	2	1	-
Extensive wash (C6)	1	1	-

As can be seen in Table 4.18, it was possible to detect crystalline structures that could be identified as Al-silicates and Ca-precipitates. No crystalline precipitate containing Na was clearly identified in any of the studied samples.

In the solid inlet to the Fe separation step, it was possible to detect at least four types of crystalline structures. Due to their chemical composition, three structures were identified as Al-silicates and one as a Ca-precipitate. The Ca-precipitate was most likely a type of Ca-phosphate.

In the filter cake obtained after normal washing (cycle 5), at least two types of Al-silicates as well as one type of Ca-precipitate were identified. One of the Al-silicate structure was of the same chemical composition as one of the structures identified in the solid inlet. The Ca-precipitate was most likely a Ca-phosphate and also of the same chemical composition as found in the solid inlet.

In the filter cake obtained after extensive washing (cycle 6), at least one type of Al-silicates and one type of Ca-precipitate were identified. The Al-silicate structure was of the same chemical composition as the Al-silicate found in both the solid inlet and the filter cake after normal washing. The Ca-precipitate was also of the same chemical composition as the Ca-phosphate in the two other samples.

5
Discussion

In the first part of this chapter, important sources of errors related to the choice of methods are briefly discussed. The following discussion mainly covers the behaviour and influence of washing conditions on the filter cake as well as the filter cake components. The Al-silicates have been investigated in more detail and is therefore discussed to a larger extent. The results from the acidic exposure is also discussed as a support to other findings. In the end of the chapter, suggestions of future work are proposed.

5.1 Sources of error due to choice of methods

Since the main objectives of the experiments were to produce a representative filter cake at normal and extensive washing conditions, some sources of error that possibly affected these results are important to evaluate.

5.1.1 Deviations from the large scale process

The exclusion of the artificial alkaline solution in the Fe separation step removed the errors related to the undesired Al-precipitate that was formed in the filter cake. Most importantly, the noticed precipitation around the Fe-precipitates could have affected the accumulation of Na in relation to these particles, meaning that these results possibly would have been lost. However, some streams present in the large scale process were removed which means that the total concentration of some elements in the reactor are not as representative of the large scale process as first desired which in turn increases the consumption of NaOH. The same conclusions can be drawn regarding filtration of precipitates in the acidic filtrate and wash water from the ash leaching discovered when the cycles were restarted without artificial alkaline solution as well as the early exclusion of the artificial acidic solution. Some elements that should be present are lost but the overall result is considered to be a better representation of the process compared to including undesired precipitates that should not be present as a solid compound in the process.

5.1.2 Deviations in cycles with varying washing conditions

Filter cakes from different washing conditions could only be collected, analysed (ICP-MS, SEM-EDS, XRD) and compared from different cycles. Since some chemicals were added by pH, and not by specific amounts, the conditions under which the cakes have been formed are not exactly the same. This means that some differences between the filter cakes can be caused by the difference in reaction conditions and not the washing itself. Another factor that can influence the comparison is differences in filter cake composition with respect to particle types that in turn can lead to differences in Na losses and washing performance. An increase of some element in the inlet can also results in a lower Na content in the filter cake. However, the only fresh chemical added to the reactor is NaOH and the decrease in Na can not reasonably be caused by an increase in inlet composition.

5.1.3 Deviations due to precision of analytical methods

All methods used in this work (mass, volume, DS measurement) as well as the analytical techniques (ISP-MS, ICP-AES) have a certain precision. This has to be taken into account when using them for the construction of the mass balance for Na since it affects the reliability of the results, especially when different instruments with varying accuracy are used in the same evaluation. For both cycle 5 with normal washing and cycle 6 with extensive washing, mass balances were constructed based on the analyses of all inlet and outlet streams, both solid and liquid. The deviation between total Na inlet and total Na outlet was 2.6 and 2.7 of the inlet. For cycle 0, only liquid analyses of the Na content was available. For this cycle, a low filtrate concentration compared to the other cycles can be noted in Table 4.4. This corresponds to a significantly larger Na loss to the filter cake which either is an indication of a measurement error in the liquid analyses for this cycle or that high amounts of Na are lost to the cake during the initiation. However, since the aim was to study Na losses under steady state operation representative to the large scale process, this has not been investigated further.

5.2 Evaluation of sodium losses and washing

The influence of washing on the Na losses to the filter cake in the Fe separation step was investigated by constructing a mass balance for cycle with normal and extensive washing. The washing behaviour was evaluated by constructing washing curves based on different wash water ratios. The obtained results related to washing are discussed in this section.

5.2.1 Sodium losses in the iron separation step

The estimations of Na losses to the filter cake, based on the cake composition analysis with ICP-MS as well as the mass balance, clearly showed an effect of extensive washing (section 4.3). Therefore, it can be concluded that it is possible to reduce the amounts of Na trapped in the filter cake by increasing the washing. Yet, at the cost of large wash water expenses.

When evaluating the effect of washing between normal washing (cycle 5) and extensive washing (cycle 6), a relatively similar reduction of Na was obtained based on the Na concentration in the filter cake (ICP-MS) and the result obtained from the mass balance. According to the filter cake concentration, extensive washing decreased the Na losses by 38% and the mass balance showed a reduction of 46% (from 5.51 wt% at cycle 5 to 3.0 wt% at cycle 6 compared to the total inlet of Na). However, it is also seen in both results (Table 4.5 and Figure 4.2), that a small amount of Na was still left in the filter cake, even after extensive washing (WW-ratio of 6.79). This implies that it is difficult to fully reduce the amount of Na trapped in the filter cake by only extended washing, which further indicate that the washing capacity is somehow limited.

Further, the effect of acidic conditions on the release of Na from the filter cake was evaluated. As illustrated in Figure 4.3, the majority of the Na trapped in the filter cake from cycle 5 was released in the acidic conditions. Thus, it is clear that the Na trapped in the filter cake can be made almost fully accessible at low pH. At the same time, the acidic exposure of Al-silicates showed that they were kept undissolved in acidic conditions. Therefore, it is believed that the acidic filter cake obtained from the acidic exposure of the filter cake, also is dominated by Al-silicates. Since almost all Na were released from the filter cake during the acidic exposure, the majority of the Na losses are most likely not related to the Al-silicates (left as a filter cake). Instead the losses are related to the other cake components.

To conclude, it is possible to reduce the amounts of Na trapped in the filter cake by increasing the washing. Yet, the washing capacity is somehow limited and the increased washing is at the cost of a large wash water consumption. Further, the majority of the Na losses is mostly related to other cake components than the Al-silicates.

5.2.2 Washing behaviour of the filter cake

The washing curve displayed in Figure 4.4 also shows that most of the accessible Na contained in the mother liquor has been washed out and indicates that some kind of equilibrium has been reached. It should however be noted that this washing curve only represents the washing behaviour of the filter cake on this particular semi-pilot scale. Dispersion was observed from a wash water ratio of 0.91 to a wash water ratio of 2.26 which means the washing becomes less efficient at larger wash water ratios than normal washing conditions [32]. Nevertheless, the washing with a cylinder on a Büchner funnel is most likely deviating significantly from a large scale washing

process meaning that the corresponding point on a larger scale is believed to be lower. These washing results should therefore not be directly used for the larger scale. Instead, only the overall behaviour of the system can be observed. To find the corresponding point for the large scale process, additional tests on this scale will be needed. In such study, the optimisation should also include the cost of NaOH-makeup and wash water.

Another aspect to mention is the establishment of the washing curve by the use of filtrate and wash water concentrations. Theoretically, a more correct result would have been obtained by tracking the real concentration of the filter cake for each wash water ratio [10]. Since the amount of cake was limited and the initial concentration of Na in the cake was unknown, this was not possible.

5.3 Behaviour of individual particles

In general, three main particles containing Na was found in the filter cake regardless of washing conditions. Most of the particles were Fe-precipitates followed by Al-silicates and only a minor amount was Ca-precipitates. After the normal washing, Ca, Fe and Na were all distributed over the entire area of the EDS-mappings while Si was distinguished from the other already after normal washing. The Na distribution is more dense in certain areas after the extensive washing. These areas corresponds more to the distribution of Si (Figure 4.15) and the distribution of Fe (Figure 4.16) than to the distribution of Ca (Figure 4.17). This means that the majority of the Na trapped in the filter cake after the extensive wash is associated with Al-silicates and Fe-precipitates. The mechanisms of Na losses in the specific particles are further discussed in this section.

5.3.1 Mechanism of sodium losses to aluminium silicates

The adsorption curve in Figure 4.5 showed that adsorption onto Al-silicates is a negligible phenomena. It can therefore be concluded that adsorption on Al-silicates is not the mechanism behind the observed Na losses. However, at the same time, it can be noticed in Table 4.6 and Table 4.7, that part of the NaOH-solution was trapped in the Al-silicate filter cake during the adsorption experiments. This means that even if Na is not adsorbed onto the Al-silicates, a part of the NaOH-solution will still be trapped in the Al-silicate filter cake. This is also confirmed in Figure 4.5, where it is clear that the majority of the Na losses are related to the trapped liquid and not the adsorption.

According to the results from point analysis with EDS in Table 4.17, the mean atomic concentration of Na in Al-silicates in the solid inlet was 10%. By comparing this value with the composition of the filter cake after normal washing in the same table, it is seen that the mean atomic concentration of Na in Al-silicates in cycle 5 has increased to 17% during the Fe separation step. This again shows that the

Al-silicates somehow are increasing their content of Na during the Fe separation step. Since, as already stated, no adsorption occurs, this result support the idea of trapped liquid since the concentration of Na is higher.

In the washing curves for the Al-silicates in Figure 4.6, it is seen that they are approaching zero at a wash water ratio of 5, which means that Na no longer is washed out. Further, the overall result in Table 4.9 indicates that very little Na was left in the Al-silicates after washing at a wash water ratio of 5. This implies that the Al-silicates are easy to wash. The effect of washing on Al-silicates is also distinct when comparing the mean atomic concentration of Na after normal washing with extensive washing in Table 4.17, based on EDS analysis. It is seen that the mean atomic concentration clearly has decreased from 17% at normal washing to 11% after extensive washing. From the results, a clear effect of washing can be noticed, which means that Na is possible to wash out from the Al-silicates. At the same time, by comparing the amounts of Na in Al-silicates in the solid inlet (10%) to after extensive washing (11%), it can be seen that the amounts of Na is almost equal. Therefore, the results highly indicate that extensive washing is sufficient for removal of Na, where it is possible to almost reduce the amounts of Na to the inlet level. However, the reduction of Na losses is at the cost of additional wash water expenses.

By instead looking at the results from the acidic exposure experiment of Ads-6 (Table 4.9), a very small release of Na from the solid cake can be noticed. This could imply that the small amounts of Na trapped in the particles are difficult to access. Yet, since there is a large deviation of Na trapped in the particles after washing in Ads-6 compared to the other samples, it is difficult to fully trust the effect of acidic treatment. Therefore, in order to understand the behaviour completely, the acidic exposure experiments should be repeated for several samples.

To conclude, Na is not adsorbed to the surface of Al-silicates, instead the particles seems to trap some of the liquid into the pore system. However, it is possible to release a majority of Na from the Al-silicates with extended washing.

5.3.2 Mechanism of sodium losses to other cake components

Table 4.17 indicates that some Na is washed out from Fe-precipitates during the extensive wash (27% compared to normal washing) but the main part is still present in the particles. It also shows that Fe-precipitates are releasing the smallest relative amount of Na during extensive washing. This shows that Fe-precipitates to a large extent is responsible for the Na losses to the filter cake that cannot be removed by washing. However, the mechanisms cannot be determined from the experiment performed. Further observations of the Fe-precipitates would be needed to determine the washing limitation of these particles and its causes.

According to the discussion in section 5.3.1, the released Na from the filter cake in acid does not come from the Al-silicates but from Fe-precipitates and/or Ca-precipitates. Since the Ca-precipitates are present only in small amounts, the Fe-

precipitates are the main contributor. It is possible that an adsorption equilibrium between Na and Fe-precipitates have been affected by the change in pH [33] or that the dissolution of the cake releases Na trapped inside pores or from the particles in contact [10],[32]. Since these particles appeared to be rather compact, it is likely that some is trapped between the particles. However, Na appeared, in some areas, to be present over entire Fe-precipitate particles (Figure 4.16) suggesting that it is attracted to the entire particle surface, for instance by adsorption. Finally, the presence of an insoluble compound between Fe and Na cannot be entirely excluded. These phenomenons can, however, only be confirmed by performing additional washing experiments with pure Fe-precipitates. It would also be possible to perform thermodynamic equilibrium calculations and diffusion time estimations to support the findings and estimate adsorption and washing limitations further [10].

Finally, the mappings of Ca (Figure 4.14 and Figure 4.17) shows that Ca is washed from most particles during the extensive washing. The Ca left in the cake thereafter is mainly associated with P in the Ca-precipitates (Appendix C). These results aligns with the washing results for Ca-precipitates from Table 4.17 which shows that 76% of the Na present in the filter cake after normal washing is washed out during the extensive washing. This result has also been observed in another study showing that Na associated to Ca-phosphates of the same structure are rather easily washed out or removed by acid treatment [60]. Given these results and the additional fact that the Ca-precipitates is only a minor component of the filter cake, it can be concluded that these particles cannot be the main contributor to the Na losses.

In conclusion, Fe-precipitates are the particles least affected by the extensive washing. The main part of Na associated to the Fe-precipitates after the extensive wash was mainly believed to be trapped as adsorbed impurities or between particles. Some losses can possibly also be located in isolated pores that cannot be targeted by the wash water. However, a further investigation of the mechanisms behind the Na trapped in Fe-precipitates will be needed to draw more certain conclusions.

5.4 Filter cake structures

No crystalline compounds with Na could clearly be detected with XRD. Instead, the main crystalline compounds that are most likely present are Ca-phosphate and Al-silicates. The presence of Al-silicates is supported by previous knowledge of the process step as well as the SEM-EDS analysis revealing clear structures of Al-silicates. The Ca-phosphate presence is supported by the observed crystalline structures in the SEM of particles containing mainly Ca and P. Their phase distribution can be further studied in Appendix C. In addition, Ca-phosphate has previously been formed when NaOH has been added during P recovery from sewage sludge ash [25].

The presence of non-crystalline Na-compounds cannot be confirmed or excluded as a possibility from the analyses performed. Hence, insoluble Na-compounds in other forms might still be present in the filter cake. Since no structures of the Al-silicates with Na were detected, even though it was seen in the SEM-EDS, other crystalline compounds of Na can also have been present in similar lower concentrations. This can nonetheless not be the main cause of the Na losses. Na was also noticed over the entire area in the mappings of the filter cake after normal washing (Figure 4.12). This makes it more likely to believe that the main part of Na is present in ionic form. However, this is the case for almost all elements which makes it difficult to draw any conclusions. Further, since the mechanism of the Na losses to Fe-precipitates have not been discovered, the possibility of a compound with Fe and Na cannot be excluded. A further investigation of pure Fe-precipitate could help to answer the question.

5.5 Future work

Due to limitations of this thesis work, only a few aspects have been investigated. Together with the obtained results from the project, there are several aspects of interest to further investigate in future studies.

The adsorption experiments in this study were limited to only Al-silicates. Since the results were able to answer important questions regarding the behaviour of the Al-silicates in this system, it is of great interest to perform similar studies on only Fe-precipitates as well. A similar experiment on adsorption of Na onto Fe-precipitates will allow to evaluate if adsorption could be the reason to the amounts of Na trapped in the Fe-precipitates, found in EDS studies.

To fully understand the limitations of the filter cake washing, it would be desired to perform a washing experiment on only Fe-precipitates to compare the washing behaviour of these particles with the washing behaviour of the Al-silicates. It would also be of interest to perform the extensive washing experiment on a larger scale to understand the washing performance, but also be able to evaluate the optimal wash water ratio in real washing conditions.

Since the washing experiment showed that extensive washing reduces the Na losses, it would be of interest to further evaluate the optimal washing procedure by including the cost perspective as well. This is since expensive washing naturally results in increased costs for equipment and operation. In order to have a functional and economical washing, it is necessary to find an optimum where the cost for Na make-up and the cost of washing are in balance. Additionally, it could also be possible to include temperature of the wash water as a parameter and evaluate the effect of it on the release of Na from the filter cake. It could be of certain interest since temperature for example can affect a possible adsorption equilibrium. However, a cost optimisation with heating of wash water would also be necessary to add, if desired results are obtained when using heated wash water.

6
Conclusions

In the present work, Na losses to the filter cake in the separation of Fe in the Ash2Phos process have been investigated. Experiments on semi-pilot scale have been conducted in order to reproduce the process step in a modified form and filter cakes have been washed with normal washing conditions (wash water ratio = 2.33) and extensive washing conditions (wash water ratio = 6.79). Additional laboratory experiments have also been conducted to support the findings. Samples of solid and liquid streams have been collected and analysed mainly with ICP-AES, ICP-MS, SEM-EDS and XRD. Three main particles with Na in the filter cake were found: Fe-precipitates and Al-silicates and Ca-precipitates. Based on the obtained results and discussion, several conclusions regarding the Na losses can be drawn which are listed below.

- Extensive washing increases the Na removal from the filter cake, however, only to a limited extent and to the cost of a significant increase in wash water consumption.
- On the semi-pilot scale investigated, optimal washing is obtained at a wash water ratio around 2.3. The corresponding point on a larger scale is believed to be lower due to the non-ideal washing procedure.
- Ca-precipitates are only a minor cake component which makes them a small contributor to the losses. Furthermore, these losses can rather easily be prevented by additional washing.
- Na is not adsorbed onto Al-silicates but the particles can trap some of the liquid which contains Na. However, since this liquid is accessible for washing, the Na losses to Al-silicates can easily be prevented by extended washing.
- Fe-precipitates are the largest contributor to the Na losses and are only affected by washing to a limited extent. This indicates that some mechanism which makes the Na inaccessible for washing are responsible for the main trapping. Likely causes are adsorption of Na onto the Fe-precipitates or trapping in the contact area between particles. To draw more exact conclusions, additional adsorption and washing experiments of pure Fe-precipitates should be conducted in future studies.
- The washing behaviour of the filter cake should be investigated on a larger scale to obtain the corresponding behaviour of the real system. Further optimisation of the washing should also include the cost of NaOH-makeup, wash water and other factors such as washing temperature.

Bibliography

[1] P. Withers, "Closing the phosphorus cycle," *Nat Sustain*, vol. 2, pp. 1001–1002, 2019. DOI: 10.1038/s41893-019-0428-6.

[2] L. Egle, H. Rechberger, J. Krampe, and M. Zessner, "Phosphorus recovery from municipal wastewater: An integrated comparative technological, environmental and economic assessment of P recovery technologies," *Science of The Total Environment*, vol. 571, pp. 522–542, 2016. DOI: 10.1016/j.scitotenv.2016.07.019.

[3] IFA, *350 years of phosphorus - phosphate rock*, 2019. [Online]. Available: https://www.fertilizer.org/Public/Stewardship/Publication_Detail.aspx?SEQN=5808&PUBKEY=7F347ACA-B95E-4EA6-A3C9-93F79F36B47D, [Accessed 2 Feb. 2021].

[4] L. W. Marissa A. de Boer and J. C. Slootweg, "Phosphorus: Reserves, production, and applications," in *Phosphorus Recovery and Recycling*, H. Ohtake and S. Tsuneda, Eds. Springer Singapore, 2019, ch. 5, pp. 75–100. DOI: 10.1007/978-981-10-8031-9.

[5] H. Ohtake and S. Tsuneda, "Preface," in *Phosphorus Recovery and Recycling*, H. Ohtake and S. Tsuneda, Eds. Springer Singapore, 2019, p. xi. DOI: 10.1007/978-981-10-8031-9.

[6] H. Kirchmann, G. Borjesson, T. Katterer, and Y. Cohen, "From agricultural use of sewage sludge to nutrient extraction: A soil science outlook.," *Ambio*, no. 2, pp. 143–154, 2017. DOI: 10.1007/s13280-016-0816-3.

[7] M. C. e. a. Collivignarelli, "Legislation for the reuse of biosolids on agricultural land in europe: Overview," *Sustainability*, vol. 11, p. 6015, 2019. DOI: 10.3390/su11216015.

[8] S. Petzet, B. Peplinski, S. Y. Bodkhe, and P. Cornel, "Recovery of phosphorus and aluminium from sewage sludge ash by a new wet chemical elution process (sesal-phos-recovery process)," *Water Science and Technology*, vol. 64, no. 3, pp. 693–699, 2011. DOI: 10.2166/wst.2011.682.

[9] EasyMining, *Ash2phos*. [Online]. Available: https://www.easymining.se/technologies/ash2phos/, [Accessed 2 Nov. 2020].

[10] S. Seupel and U. A. Peuker, "Displacement washing of filter cakes from porous particles," *Separation and Purification Technology*, p. 118 129, 2021. DOI: 10.1016/j.seppur.2020.118129.

[11] USGS, *Mineral commodity summaries of phosphate rock 2021*, 2021. [Online]. Available: https://pubs.usgs.gov/periodicals/mcs2021/mcs2021-phosphate.pdf, [Accessed 17 Feb. 2021].

[12] UNEP and IFA, *Environmental aspects of phosphate and potash mining*. France: UNEP and IFA, 2001. [Online]. Available: http://digitallibrary.un.org/record/476520, [Accessed 23 Jan. 2021].

[13] S. Karlsson, "Human-caused material flows," in *Man and material flows: Towards sustainable materials management*, ser. A sustainable Baltic region. Sweden: Baltic University Programme, Uppsala University, 1997, ch. 3, pp. 17–21. [Online]. Available: https://research.chalmers.se/publication/505263/file/505263_Fulltext.pdf, [Accessed 17 Feb. 2021].

[14] Commission of European Union, *Communication from the commission to the european parliament, the council, the european economic and social committee and the committee of the regions. critical raw materials resilience: Charting a path towards greater security and sustainability*, 2020. [Online]. Available: https://eur-lex.europa.eu/legal-content/EN/TXT/?uri=CELEX:52020DC0474, COM/2020/474.

[15] Britannica, The Editors of Encyclopaedia, "Phosphorus - chemical element," in *Encyclopedia Britannica*. 2019. [Online]. Available: https://www.britannica.com/science/phosphorus-chemical-element, [Accessed 17 Feb. 2021].

[16] K. Schrödter, G. Bettermann, T. Staffel, F. Wahl, T. Klein, and T. Hofmann, "Phosphoric acid and phosphates," in *Ullmann's Encyclopedia of Industrial Chemistry*, C. L. et al, Ed. Wiley-VCH Verlag GmbH Co, 2008, pp. 679–721. DOI: 10.1002/14356007.a19_465.pub3.

[17] I. Twardowska, K.-W. Schramm, and K. Berg, "Sewage sludge," in *Solid Waste: Assessment, Monitoring and Remediation*, I. Twardowska, Ed., ser. Waste Management Series. Elsevier, 2004, vol. 4, ch. III.4, pp. 239–295. DOI: 10.1016/S0713-2743(04)80013-8.

[18] A. Ambulkar and J. A. Nathanson, "Wastewater treatment," in *Encyclopedia Britannica*. 2021. [Online]. Available: https://www.britannica.com/technology/wastewater-treatment, [Accessed 19 Feb. 2021].

[19] W. Schipper, "Success factors for implementing phosphorus recycling technologies," in *Phosphorus Recovery and Recycling*, H. Ohtake and S. Tsuneda, Eds. Springer Singapore, 2019, ch. 6, pp. 101–130. DOI: 10.1007/978-981-10-8031-9.

[20] S. Wick, B. Baeyens, M. Marques Fernandes, and A. Voegelin, "Thallium adsorption onto illite," *Environmental Science & Technology*, vol. 52, no. 2, pp. 571–580, 2018. DOI: 10.1021/acs.est.7b04485.

[21] Y. Al-Degs, M. Khraisheh, and M. Tutunji, "Sorption of lead ions on diatomite and manganese oxides modified diatomite," *Water Research*, vol. 35, no. 15, pp. 3724–3728, 2001. DOI: 10.1016/S0043-1354(01)00071-9.

[22] M. Alkan and M. Doğan, "Adsorption of copper(ii) onto perlite," *Journal of Colloid and Interface Science*, vol. 243, no. 2, pp. 280–291, 2001. DOI: 10.1006/jcis.2001.7796.

[23] M. Irani, M. Amjadi, and M. A. Mousavian, "Comparative study of lead sorption onto natural perlite, dolomite and diatomite," *Chemical Engineering Journal*, vol. 178, pp. 317–323, 2011. DOI: 10.1016/j.cej.2011.10.011.

[24] A. Prasetya, P. Prihutami, A. D. Warisaura, M. Fahrurrozi, and H. T. B. Murti Petrus, "Characteristic of hg removal using zeolite adsorption and echin-

odorus palaefolius phytoremediation in subsurface flow constructed wetland (ssf-cw) model," *Journal of Environmental Chemical Engineering*, vol. 8, no. 3, p. 103 781, 2020. DOI: 10.1016/j.jece.2020.103781.

[25] L. Fang, J.-s. Li, S. Donatello, C. Cheeseman, Q. Wang, C. S. Poon, and D. C. Tsang, "Recovery of phosphorus from incinerated sewage sludge ash by combined two-step extraction and selective precipitation," *Chemical Engineering Journal*, vol. 348, pp. 74–83, 2018. DOI: 10.1016/j.cej.2018.04.201.

[26] R. M. Harrison, "Chemistry of freshwaters," in *Principles of Environmental Chemistry*. UK: Royal Society of Chemistry, 2007, ch. 3, pp. 80–169. [Online]. Available: https://app.knovel.com/hotlink/toc/id:kpPEC00004/principles-environmental/principles-environmental, [Accessed 27 Apr. 2021].

[27] J. C. Crittenden, R. R. Trussell, D. W. Hand, K. J. Howe, and G. Tchobanoglous, "Principles of chemical reactions," in *MWH's Water Treatment - Principles and Design (3rd Edition)*. United states: John Wiley Sons, 2012, ch. 5, pp. 225–285. [Online]. Available: https://app.knovel.com/hotlink/toc/id:kpMWHWTPD1/mwh-s-water-treatment/mwh-s-water-treatment, [Accessed 27 Apr. 2021].

[28] T. Biscontini, "Solubility," *Salem Press Encyclopedia of Science*, 2019. [Online]. Available: https://search.ebscohost.com/login.aspx?direct=true&db=ers&AN=98402407&site=eds-live&scope=site&authtype=guest&custid=s3911979&groupid=main&profile=eds, [Accessed 27 Apr. 2021].

[29] P. Atkins, L. Jones, and L. Laverman, "Aqueous equilibria," in *Chemical Principles: The Quest for Insight*, 6th ed. W.H. Freeman and Company, 2013, ch. 13, pp. 519–560, ISBN: 978-1-4641-2467-9.

[30] S. Petzet, B. Peplinski, and P. Cornel, "On wet chemical phosphorus recovery from sewage sludge ash by acidic or alkaline leaching and an optimized combination of both," *Water Research*, vol. 46, no. 12, pp. 3769–3780, 2012. DOI: 10.1016/j.watres.2012.03.068.

[31] K.-i. Sonoda, "Alkaline leaching of phosphate from sewage sludge ash," in *Phosphorus Recovery and Recycling*, H. Ohtake and S. Tsuneda, Eds. Springer Singapore, 2019, ch. 8, pp. 143–148. DOI: 10.1007/978-981-10-8031-9.

[32] H. Anlauf, "Particle washing," in *Wet Cake Filtration - Fundamentals, Equipment, and Strategies*. Germany: John Wiley Sons, 2019, ch. 7, pp. 175–202. [Online]. Available: https://app.knovel.com/hotlink/toc/id:kpWCFFES01/wet-cake-filtration-fundamentals/wet-cake-filtration-fundamentals, [Accessed Mar. 2021].

[33] S. Noerpel, V. Siauw, and H. Nirschl, "Filter cake washing of mesoporous particles," *Chemical Engineering & Technology*, vol. 35, no. 4, pp. 661–667, 2012. DOI: 10.1002/ceat.201100467.

[34] B. Perlmutter, "Introduction," in *Solid-Liquid Filtration:Practical Guides in Chemical Engineering*. UK: Elsevier Science Technology, 2015, ch. 1, pp. 1–18. [Online]. Available: https://ebookcentral.proquest.com/lib/chalmers/reader.action?docID=1956679, [Accessed Mar. 2021].

[35] H. Anlauf, "Cake structure characterization," in *Wet Cake Filtration - Fundamentals, Equipment, and Strategies*. Germany: John Wiley Sons, 2019,

ch. 3, pp. 41–55. [Online]. Available: https://app.knovel.com/hotlink/toc/id:kpWCFFES01/wet-cake-filtration-fundamentals/wet-cake-filtration-fundamentals, [Accessed Mar. 2021].

[36] E. Tarleton and R. J. S. Wakeman, "Pretreatment of suspensions," in *Solid/Liquid Separation - Equipment Selection and Process Design*. UK: Elsevier, 2007, ch. 3, pp. 126–151. [Online]. Available: https://app.knovel.com/hotlink/toc/id:kpSLSESPD6/solid-liquid-separation/solid-liquid-separation, [Accessed 17 Feb. 2021].

[37] J. Wang and X. Guo, "Adsorption isotherm models: Classification, physical meaning, application and solving method," *Chemosphere*, vol. 258, p. 127 279, 2020. DOI: 10.1016/j.chemosphere.2020.127279.

[38] M. A. Al-Ghouti and D. A. Da'ana, "Guidelines for the use and interpretation of adsorption isotherm models: A review," *Journal of Hazardous Materials*, vol. 393, p. 122 383, 2020. DOI: 10.1016/j.jhazmat.2020.122383.

[39] W. Stumm, *Chemistry of the solid-water interface: Processes at the mineral-water and particle-water interface in natural systems*. United States: John Wiley & Sons, 1992, ISBN: 9780471576723.

[40] F. M. M. Morel and J. G. Hering, *Principles and applications of aquatic chemistry*. United States: John Wiley & Sons, 1993, ISBN: 9780471548966.

[41] D. C. Harris, "Fundamentals of spectrophotometry," in *Quantitative chemical analysis*. 8th ed. United States: Freeman and Co, 2010, ch. 17, pp. 393–418, ISBN: 9781429218153.

[42] Hach Sverige, *Järnkyvettest, 0,2-6,0 mg/L Fe, 25 tester | Hach Sverige - Översikt*. [Online]. Available: https://se.hach.com/jarnkyvettest-0-2-6-0-mg-l-fe-25-tester/product?id=26370291844&callback=qs, [Accessed 9 Apr. 2021].

[43] ——, *Aluminiumkyvettest, 0,02-0,5 mg/L Al, 24 tester | Hach Sverige - Översikt*. [Online]. Available: https://se.hach.com/aluminiumkyvettest-0-02-0-5-mg-l-al-24-tester/product?id=26370270227, [Accessed 9 Apr. 2021].

[44] ——, *Ortofosfatkyvettest, 1,6-30 mg/L xn–PO-ucu-P, 25 tester | Hach Sverige - Översikt*. [Online]. Available: https://se.hach.com/ortofosfatkyvettest-1-6-30-mg-l-po-p-25-tester/product?id=26370270203, [Accessed 9 Apr. 2021].

[45] D. C. Harris, "Atomic spectroscopy," in *Quantitative chemical analysis*. 8th ed. United States: Freeman and Co, 2010, ch. 20, pp. 479–501, ISBN: 9781429218153.

[46] G. M. Hieftje, "Atomic spectrometry," *AccessScience*, 2020. DOI: 10.1036/1097-8542.060800, [Accessed 26. Mar 2021].

[47] M. J. Cope and G. F. Kirkbright, "Some aspects of analytical atomic emission spectroscopy using inductively coupled plasma sources," *Journal of Physics E: Scientific Instruments*, vol. 16, pp. 581–588, 1983. DOI: 10.1088/0022-3735/16/7/001.

[48] S. C. Wilschefski and M. R. Baxter, "Inductively coupled plasma mass spectrometry: Introduction to analytical aspects.," *The Clinical biochemist. Reviews*, vol. 40, no. 3, pp. 115–133, 2019. DOI: 10.33176/AACB-19-00024.

[49] M. M. Bursey and T. D. Williams, "Mass spectrometry," *AccessScience*, 2020. DOI: 10.1036/1097-8542.408700, [Accessed 26 Mar. 2021].

[50] Brian J. Ford and Savile Bradbury and David C. Joy, "Scanning electron microscope," in *Encyclopedia Britannica*. 2019. [Online]. Available: https://www.britannica.com/technology/scanning-electron-microscope, [Accessed 22 Mar. 2021].

[51] L. Reimer, "Scanning electron microscope - introduction," in *Scanning Electron Microscopy: Physics of Image Formation and Microanalysis*, 2nd ed., ser. Springer series in optical sciences. New York: Springer-Verlag Berlin Heidelberg, 1998, ch. 1, pp. 1–12. DOI: 10.1007/978-3-540-38967-5.

[52] Hitachi High-Technologies Corporation, *Let's Familiarize Ourselves with the SEM!* Tokyo: Hitachi High-Technologies Corporation, 2013.

[53] S. Nasrazadani and S. Hassani, "Modern analytical techniques in failure analysis of aerospace, chemical, and oil and gas industries," in *Handbook of Materials Failure Analysis with Case Studies from the Oil and Gas Industry*, A. S. H. Makhlouf and M. Aliofkhazraei, Eds. UK: Butterworth-Heinemann, 2016, ch. 2, pp. 39–54. DOI: 10.1016/B978-0-08-100117-2.00010-8.

[54] L. Reimer, "Elemental analysis and imaging with x-rays," in *Scanning Electron Microscopy: Physics of Image Formation and Microanalysis*, 2nd ed., ser. Springer series in optical sciences. New York: Springer-Verlag Berlin Heidelberg, 1998, ch. 10, pp. 379–448. DOI: 10.1007/978-3-540-38967-5.

[55] D. N. Lumsden, "X-ray powder diffraction.," *Salem Press Encyclopedia of Science*, 2019. [Online]. Available: https://search.ebscohost.com/login.aspx?direct=true&db=ers&AN=88806811&site=eds-live&scope=site&authtype=guest&custid=s3911979&groupid=main&profile=eds, [Accessed 24 Mar. 2021].

[56] E. F. Paulus and A. Gieren, "Structure analysis by diffraction," in *Ullmann's Encyclopedia of Industrial Chemistry*, C. L. et al, Ed. American Cancer Society, 2002. DOI: 10.1002/14356007.b05_341.

[57] Hydragyrum, *File:Bragg diffraction 2.svg*, (CC BY-SA 3.0, https://creativecommons.org/licenses/by-sa/3.0/deed.en), 2011. [Online]. Available: https://commons.wikimedia.org/wiki/File:Bragg_diffraction_2.svg.

[58] C. SuryanarayanaM and G. Norton, "X-rays and diffraction," in *X-Ray Diffraction: A Practical Approach*. United states: Springer, Boston, MA, 1998, ch. 1, pp. 3–19. DOI: 10.1007/978-1-4899-0148-4.

[59] *Dr3900 laboratorie-spektrofotometer för vattenanalys*. [Online]. Available: https://se.hach.com/family-print.pdf.jsa?pageNumber=1&pageSize=10&sortBy=sequence&defaultSortBy=sequence&sortDirection=&sortDiscriminator=&productCategoryId=24821604193&price=&seeMoreFilter=&secondPageNumber=1&topSectionOpen=0&productFamilyAttributes1=&productFamilyAttributes1Discr=24761219373&productFamilyAttributes2=&productFamilyAttributes2Discr=24761219134&productFamilyAttributes3=&productFamilyAttributes3Discr=24761219039&focusResults=true, [Accessed 9 Apr. 2021].

[60] W. Schmid, M. Aia, and R. Mooney, "Study of adsorption and coprecipitation of sodium in calcium phosphates using na-22 tracer," *Journal of Inorganic and*

Nuclear Chemistry, vol. 28, no. 5, pp. 1325–1328, 1966. DOI: https://doi.org/10.1016/0022-1902(66)80461-X.

A

Cooling agent contamination during SEM-EDS sample preparation

This appendix contains mappings from SEM-EDS analysis of Na from the same filter cake but grinded with water and ethanol respectively. The mappings show the distribution of the Na over the area of the mapping. The results can be compared to investigate the influence of contamination of water in the samples. The examples is from cycle 6 of cycles with artificial alkaline solution excluded.

(a) 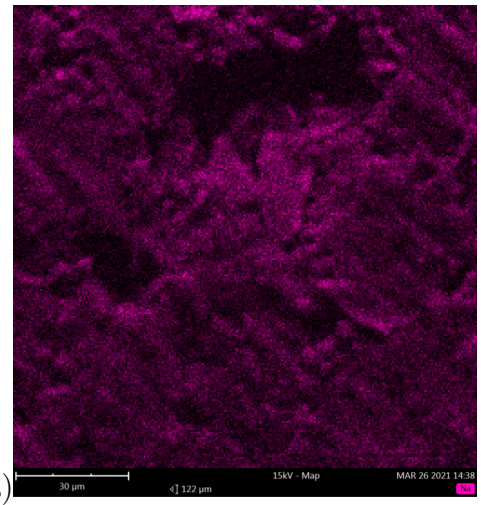

(b) 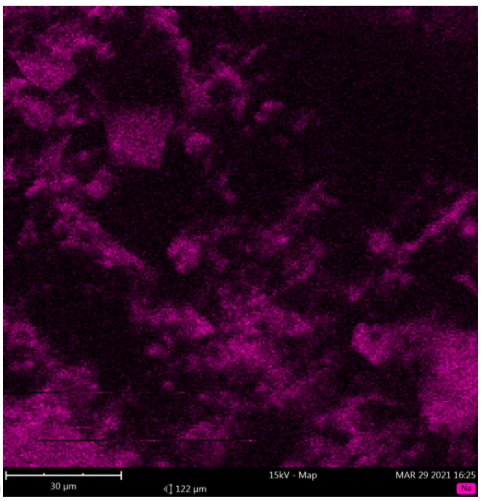

Comparison of distribution of Na when grinded with (a) water and (b) ethanol, showing the impact of water contamination.

The mappings show an Na distribution over the entire area after the polishing with water in contrast to the polishing with ethanol which resulted in a more distinct distribution in certain areas. This can indicate that the polishing with water resulted in a contamination of Na or perhaps also other water-soluble compounds in the sample.

B

Mapping areas in filter cakes from cycle 5 and 6

The mappings of the filter cake from cycle 5 and cycle 6 without artificial alkaline solution was performed on one area of each cake at a magnification of 2200x. This makes it possible to compare the distribution of different elements and search for similarities. In the following figure, the mapping areas that were used and presented in the results for cycle 5 and cycle 6, can be seen.

(a) 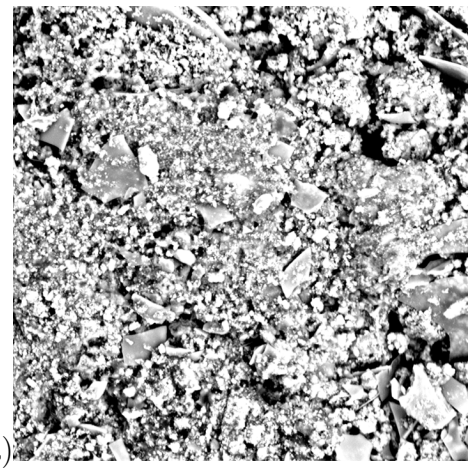 (b) 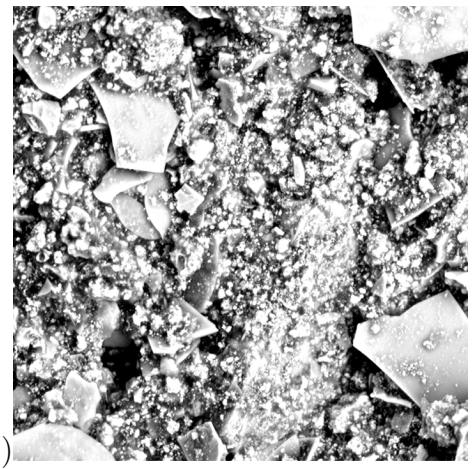

Filter cake areas used for the EDS-mappings presented in the results for (a) cycle 5 and (b) cycle 6.

C

Distribution of Ca, P, Si and Al after extensive washing

This appendix provides some additional mappings of elements from SEM-EDS analysis in the filter cake after extensive washing (wash water ratio = 6.79) that can serve as a deeper understanding of the elements distribution in the filter cake. The area of the mapping is the same as for all other figures with mappings of elements from cycle 6 with extensive washing. The figures gives an indication of other elements that are associated in the cake. In the following figure, the distribution of Ca and P in the filter cake after the extensive washing can be compared.

(a) 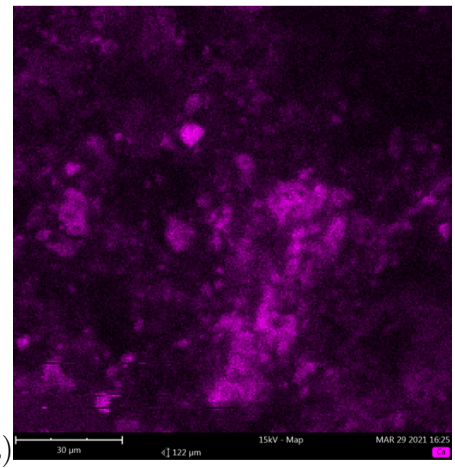

(b) 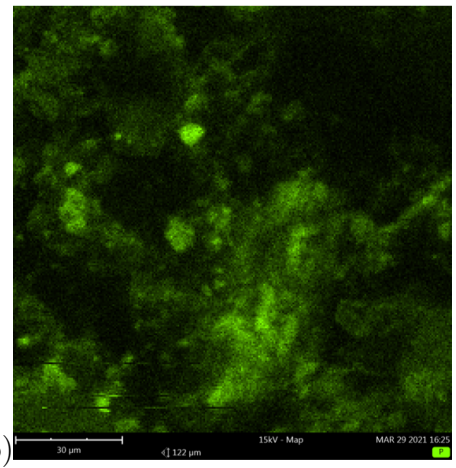

Comparison of distribution between (a) Ca and (b) P in the filter cake after extensive washing conditions grinded with ethanol showing a possible presence of Ca-phosphates in the filter cake. The distribution of both elements are more distinct after the extensive washing.

Ca and P are associated in the filter cake according to the mapping results. In the following figure, the distribution of Al and Si in the filter cake after the extensive washing can be compared. It can be seen that both Al and Si are associated with the Al-silicate particles only and are not distributed over the entire area of the mapping.

(a) 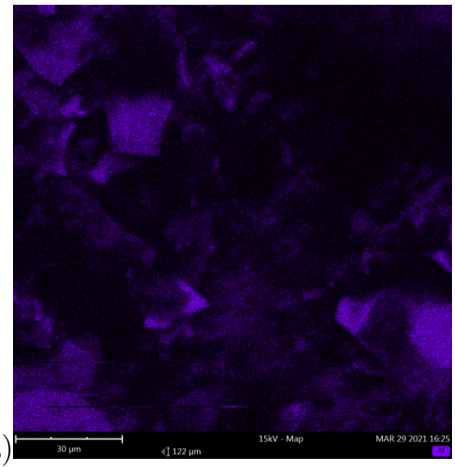

(b) 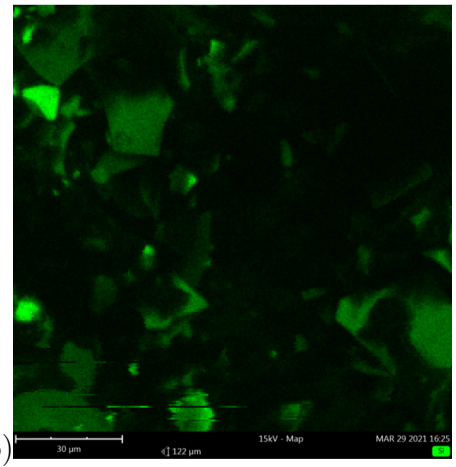

Comparison of distribution between (a) Al and (b) Si in the filter cake after extensive washing conditions grinded with ethanol showing distinct Al-silicate particles.

Al and Si are associated in the filter cake according to the mapping results. This is also an expected result since Al-silicates are known to be present in the filter cake.

DEPARTMENT OF CHEMISTRY AND CHEMICAL ENGINEERING
CHALMERS UNIVERSITY OF TECHNOLOGY
Gothenburg, Sweden
www.chalmers.se

CHALMERS
UNIVERSITY OF TECHNOLOGY